Chapter 5: The Cellular and Structural Effect of Triton X-100 and CoQ10, Alone, and in Combination as Determined by Scanning Electron Microscopy (SEM)

5.1 Introduction

Many cellular structures are so small that they can only be resolved in the electron microscope. Furthermore, it is often crucial to visualize and reconstruct the three-dimensional (3D) structure of biological tissue. Scanning electron microscopy (SEM) in which a tightly focused beam of electrons is raster-scanned over the specimen while secondary or backscattered electrons are detected, is used in biological imaging mostly as a surface visualization tool, creating a 3D appearance. The prevalent contrast mode in the SEM is the detection of so-called secondary electrons, which are low-energy electrons that are emitted when the primary electron beam strikes the sample surface, providing high-resolution imaging of fine surface morphology. The secondary-electron signal depends strongly on the orientation of the surface, leading to topographic images that characteristically resemble obliquely illuminated solid objects. The orientation of surface features influences the number of electrons that reach the secondary electron detector, which creates variations in image contrast that represents the sample's surface topography. SEM is a method for high-resolution imaging of surfaces, and the advantages over light microscopy include magnification of up to 100 000 times and much greater depth of field (Denk *et al*., 2004 and Hanke *et al*., 2006). Scanning electron microscopy is a useful method for studying the cell surface during muscle development in cell culture (Shimada, 1972).

Skeletal muscle fibers are multinucleated cells, with their numerous nuclei peripherally located just beneath the cell membrane (sarcolemma). An endomysium, whose fine reticular fibers intermingle with those of neighboring cells, surrounds each cell. Small satellite cells, which have only a single nucleus and act as regenerative cells, are located in shallow depressions on the muscle cell's surface, sharing the muscle fiber's external lamina. Much of the skeletal muscle cell is composed of longitudinal arrays of cylindrical myofibrils, each 1 to 2μm in diameter. A myofibril consists of thick

myofilaments (15nm in diameter and 1.5μm long), composed of myosin II, and thin filaments (7nm in diameter and 1.0μm long), composed primarily of actin. These extend the entire length of the cell and are aligned precisely with their neighbours. This strictly ordered parallel arrangement of the myofibrils is responsible for the cross-striations of light and dark banding that are characteristic of skeletal muscle viewed in longitudinal section. The dark bands are known as A bands (anisotropic with polarized light) and the light bands as I bands (isotropic with polarized light). The center of each A band is occupied by a pale area, the H band which is bisected by a thin M line. Each I band is bisected by a thin dark line, the Z disc. The region of the myofibril between two successive Z discs, known as a sarcomere, is 2.5μm in length and considered the contractile unit of skeletal muscle fibers. Myofibrils are held in register with one another by the intermediate filaments desmin and vimentin, which secure the periphery of the Z discs of neighbouring myofibrils to each other. These bundles of myofibrils are attached to the cytoplasmic aspect of the sarcolemma by various proteins including dystrophin, a protein that binds to actin (Gartner *et al*., 2007). Traditionally, the Z disc has been viewed as a passive constituent of the sarcomere, which is important only for the cross-linking of thin filaments and transmission of force generated by the myofilaments. During the last decade, remarkable progress has been made in deciphering the functional role of the Z disc in striated muscle. Starting from a mainly structural perception of the Z disc, the recent discovery of a progressively increasing number of “Z disc proteins” as well as novel protein-protein interactions implicated the Z disc as a nodal point in striated muscle signalling. The pivotal position of the Z disc is further underscored by the fact that cardiomyopathies and muscle dystrophies have been linked to mutations in numerous genes encoding for proteins of the Z-disc and closely adjacent structures of the myocyte (Frank *et al*., 2006).

The fine structure of the sarcolemma is similar to that of other cell membranes, but a distinguishing feature is that it is continued within the skeletal muscle fiber as numerous long, tubular invaginations that intertwine among the myofibrils, known as T tubules (transverse tubules). T tubules extend deep into the interior of the fiber and facilitate the conduction of waves of depolarization along the sarcolemma. Associated with this system of T tubules, is the sarcoplamic reticulum, which stores intracellular calcium and is maintained in close register with the A and I bands as well as with the T tubules. The sarcoplasmic reticulum forms a meshwork around each myofibril and displays dilated

terminal cisternae at each A-I junction. Two of these cisternae are always in close apposition to a T tubule, forming a triad in which a T tubule is flanked by two terminal cisternae. This arrangement permits a wave of depolarization to spread, almost instantaneously, from the sarcolemma throughout the cell, reaching the terminal cisternae, which have voltage-gated calcium release channels in their membrane. The sarcoplasmic reticulum regulates muscle contraction through the controlled sequestering and release of calcium ions within the sarcoplasm. The wave of depolarization transmitted by the T tubules triggers calcium ion release, which causes opening of the calcium release channels of the terminal cisternae, resulting in release of calcium ions into the cytosol in the vicinity of the myofibrils (Gartner *et al*., 2007).

Cardiac muscle differs from smooth and skeletal muscles in that it possesses an inherent rhythmicity as well as the ability to contract spontaneously. Although the resting volume of individual cardiac muscle cells varies, on average they are 15μm in diameter and 80μm in length. Each cell possesses a single, large, oval, centrally placed nucleus; although two nuclei are occasionally present (Gartner *et al*., 2007). The bandings of cardiac muscle are identical with those of skeletal muscle, including alternating I and A bands. Each sarcomere possesses the same substructure as its skeletal muscle counterpart; therefore, the mode and mechanism of contraction are virtually identical. The sarcoplasmic reticulum of cardiac muscle does not form terminal cisternae and is not nearly as extensive as in skeletal muscle; instead, small terminals of sarcoplasmic reticulum approximate the T tubules. These structures do not normally form a triad, as in skeletal muscle, but rather the association is usually limited to two partners, resulting in a dyad. Unlike skeletal muscle, where the triads are located at the A-I interfaces, the dyads in cardiac muscle are located in the vicinity of the Z disc. The T tubules of cardiac muscle cells are almost two and a half times the diameter of those in skeletal muscle and are lined by an external lamina. The highly specialized end-to-end junctions formed by cardiac cells are referred to as intercalated discs. The cell membranes involved in these junctions approximate each other, so that in most areas they are separated by a space of less than 15 to 20 nm. Intercalated discs have transverse portions, where fasciae adherents and desmosomes abound, as well as lateral portions rich in gap junctions. On the cytoplasmic side of intercalated discs, thin myofilaments attach to the fasciae adherens, which are analogous to Z discs. Gap junctions which function in

permitting rapid flow of information from one cell to the next, also form in regions where cells lying side by side come in close contact with each other (Gartner *et al*., 2007).

Triton X-100 is one of the most commonly used non-ionic detergents for solubilizing membrane proteins during isolation of membrane-protein complexes (Roche). Non ionic surfactants, such as Triton X-100, have been used extensively in a wide variety of biological systems for both preparative and functional studies of membrane proteins. The interaction of such micelle-forming amphiphiles with biological membranes is a highly complex process, which involves the initial insertion of individual surfactant molecules into the lipid bilayer, followed by the formation of mixed lipid-detergent micelles and even large lipoprotein bilayer discs stabilized by a pseudo-micellar annulus of detergent (Dunahay *et al*., 1984). The process culminates in the incorporation of all of the membrane components into detergent micelles (Murphy *et al*., 1985).

CoQ10 is present in the endomembranes of cells as well as in mitochondria, where it serves as a central component of the transmembrane electron transport system (Sun *et al*., 1992). Antioxidants such as CoQ10 can neutralize free radicals and reduce or even help prevent some of the damage that is caused (Al-Hasso, 2001). Coenzyme Q10 is effective in preventing protein oxidation by quenching the initiating perferryl radical and functioning as a chain-breaking antioxidant, thus preventing the process of propagation, the second phase in lipid peroxidation, where $LOO^{\cdot}$ abstracts a hydrogen atom from an additional unsaturated fatty acid, leading to $L^{\cdot}$ and lipid hyperoxide (LOOH), which can be reoxidized to $LOO^{\cdot}$, which reinitiates lipid peroxidation (Bentinger *et al*., 2007). Coenzyme Q10 is proposed to play a central role in antioxidant protection of the plasma membrane, either directly or through the regeneration of important exogenous antioxidants such as α-tocopherol and ascorbate (Gómez-Díaz *et a*l., 2000). Coenzyme Q10 can be considered as the central molecule in plasma membrane protection against lipid peroxidation because it is directly reduced by cytochrome b_5 reductase, and maintains both ascorbate and α-tocopherol in their reduced state (López-Lluch *et al*., 1999).

In order to investigate whether CoQ10 will elicit a protective effect, as described in the literature, (Papucci *et al*., 2003 and Kagan *et al*., 1999) on cells exposed to different concentrations of Triton X-100, scanning electron microscopy was used to determine

structural and morphological alterations to cell membranes exposed to increasing concentrations of Triton X-100, CoQ10 and a combination of the two substances.

In this Chapter the following research objectives were investigated:

- Investigate the ultrastructure of cardiac and skeletal muscle cells in primary culture, exposed to Triton X-100 and CoQ10, SEM.
- Determine whether CoQ10 offer any protection to cardiac and skeletal muscle cells in primary culture, ultrastructurally altered by the cell lysing properties of Triton X-100, by SEM.

5.2 Materials and Methods

Poly-L-lysine was from Sigma-Aldrich (Pty) Ltd., Midrand, South Africa. The 22mm x 22mm Menzel Glazer coverslips were from Agar Scientific, Cambridge, England.
The primary chick embryonic cardiac and skeletal muscle cell cultures were prepared as for cytotoxicity testing in Chapter 4. To examine the cardiac and skeletal muscle cell morphology and structure of the primary cultures, the primary cultures were plated at a concentration of $5x10^4$cells/ml onto the surface of Menzel Glazer glass coverslips coated with Poly-L-lysine (1ml Poly-L-lysine in 9ml sterile ddH_2O) positioned on the bottom of 24-well plates. After 72 hours of incubation the cell cultures were exposed to Triton X-100 and CoQ10, alone and in combination, for 24 hours. To determine the effect of CoQ10 on cells exposed to Triton X-100, cell cultures were pre-treated with the different concentrations of CoQ10, 0.02 – 0.2mg/ml, 2 hours prior to exposure to Triton X-100, and maintained for the rest of the 24 hours at 37°C and 5% CO_2. Samples were then prepared for detailed morphological investigation using SEM. After 86 hours in culture the medium was removed and the monolayer was washed with a phosphate buffered saline solution (PBS). The monolayer of each well was fixed with 2.5% gluteraldehyde in a 0.075M phosphate buffer pH7.4. After 90 minutes the fixative was removed and each well was washed 3 times (15 minutes each) with 0.075M phosphate buffer. Postfixation was then done for 60 minutes in a 1% osmium tetraoxide (OsO_4) solution. After postfixation each well was washed 3 times, (15 minutes each) with 0.075M phosphate buffer to remove any remaining osmium tetraoxide. Once the washing step was complete, a dehydration step took place in which each well went through serial

dehydration with ethanol, 30%, 50%, 70%, 90% and three times 100%, each dehydration step took place for 15 minutes. The coverslips were then removed from the 24-well plates and dried, by means of a CO_2 critical point drying procedure; samples were mounted and examined with a ZEISS ULTRA 55 FEG.SEM. According to Boyde *et al*., 1979, during critical point drying a sample can loose up to 20% of its volume, which is probably the reason why fine cracks and broken muscle cell tips were seen in the results of this study (Boyde *et al*., 1979). Before the samples were visualized it had to be made conductive, using ruthenium oxide (RuO_4) vapour. Depositions of the RuO_4 crystals were seen on the results and were identified by Van der Merwe (1999), as ruthenium artefacts.

5.3 Results and Discussion

The effect of Triton X-100 and CoQ10, alone, and in combination, on the cellular structure and morphology of cardiac and skeletal muscle cells, and more specifically the membranes of the cells, was determined by visualization of the high-resolution surface images produced by SEM.

5.3.1 Control Group

Skeletal and cardiac muscle cells in the control group were not exposed to either of the two substances being tested. The cell morphology, structure and membrane integrity reflect that of normal intact cells. During muscle cell differentiation many changes take place in the surface properties of the cells (Masuko *et al*., 1983). Masuko *et al*., 1983, determined that in the late G_2 phase of the cell cycle, cells have bulged in anticipation of rounding for mitosis, and many microvilli (Figure 5.1b and 5.2b, indicated by the thin white arrows), some blebs, and long slender filopodia (Figure 5.1a and 5.2 a, at bipolar ends of cells) appeared on the surfaces (Masuko *et al*., 1983). During G_1 and S, the cells are spindle-shaped with a relatively smooth surface. During the M phase cells are generally spherical and their surface is covered with numerous microvilli and some blebs (Masuko *et al*, 1983).

a)

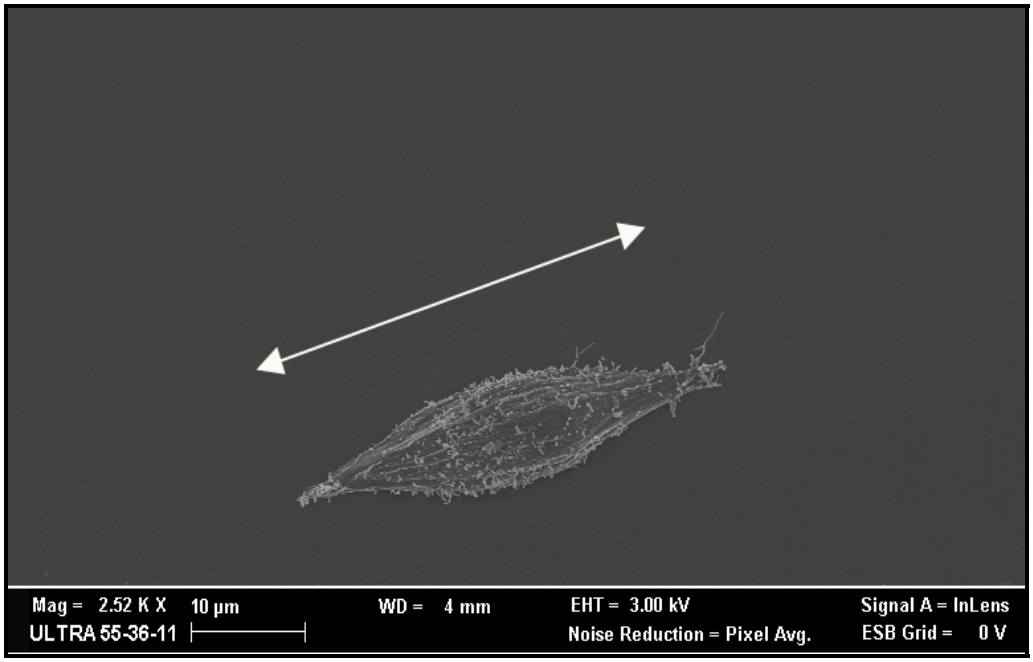

b)

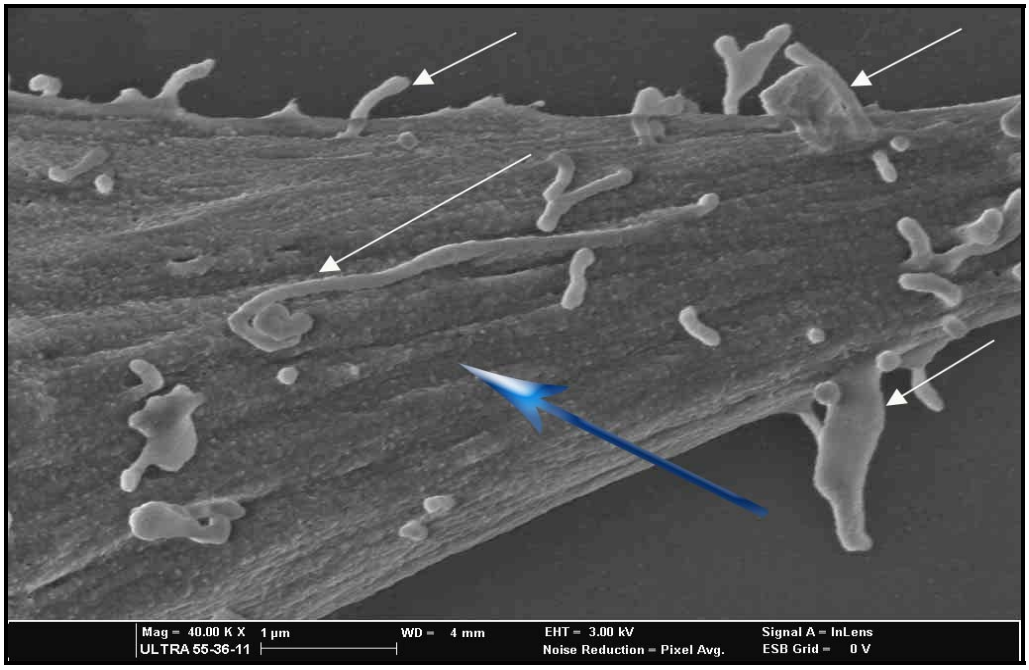

Figure 5.1: Skeletal muscle cells from the control group, at high and low magnification. Intact membranes were observed (blue arrow). **a**): Low magnification; bipolar cytoplasmic extensions become slender with filopodia extending into the substrate. **b**): High magnifications of (**a**); presence of microvilli on the membrane surface (**b** - thin white arrows).

a)

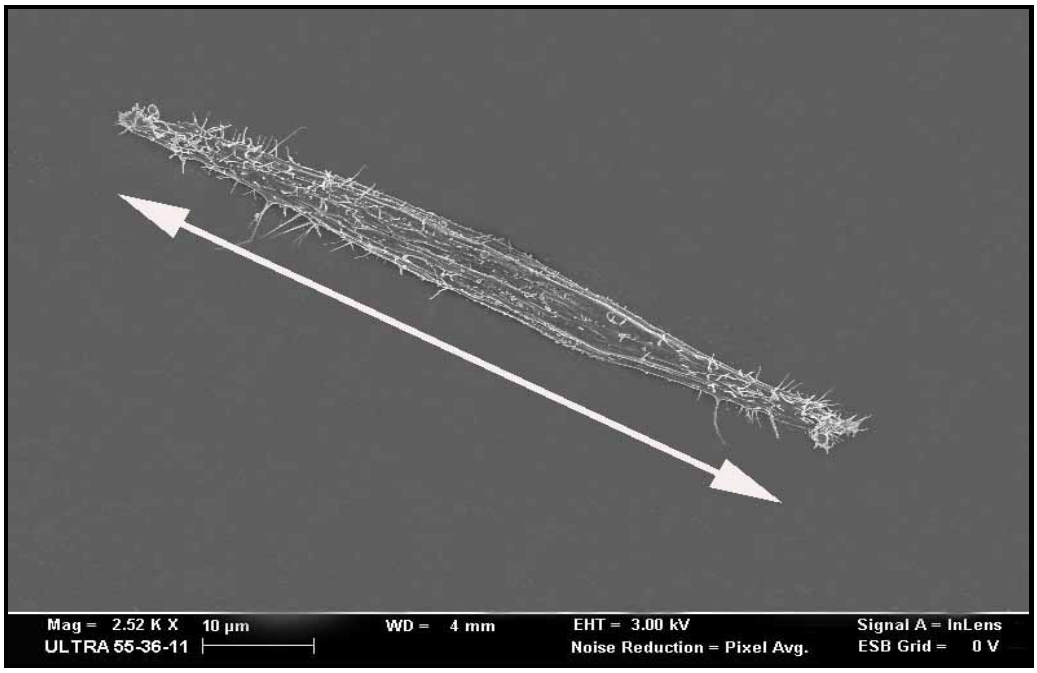

b)

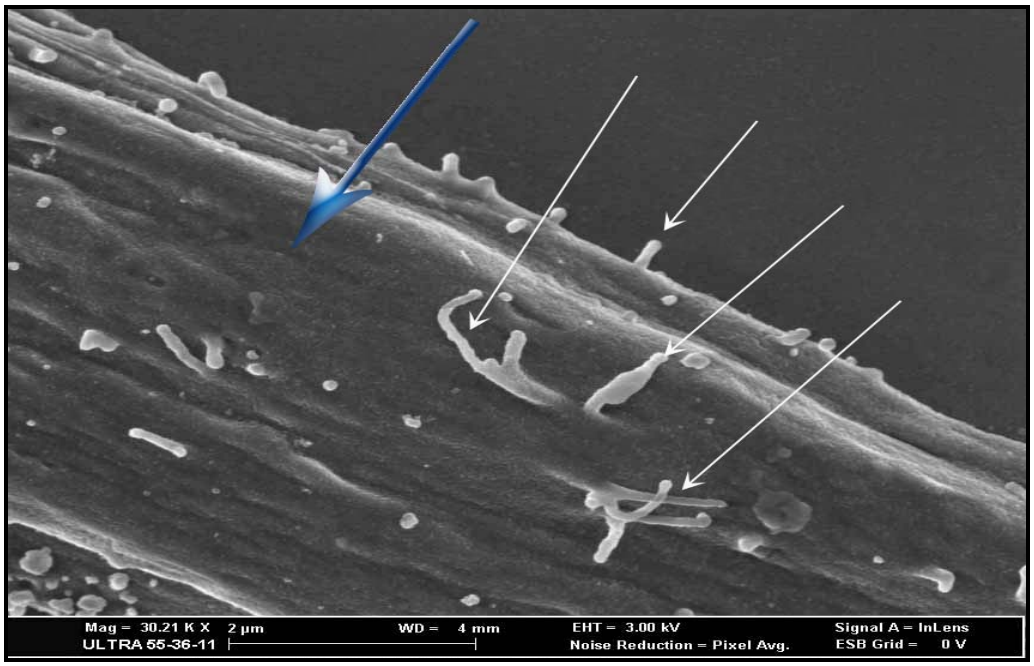

Figure 5.2: Cardiac muscle cells from the control group, at high and low magnification. Intact membranes were observed (blue arrow). **a**): Low magnification; bipolar cytoplasmic extensions become slender with filopodia extending into the substrate. **b**): High magnifications of (**a**); presence of microvilli on the membrane surface (**b** - thin white arrows).

5.3.2 Cells exposed to Triton X-100

a)

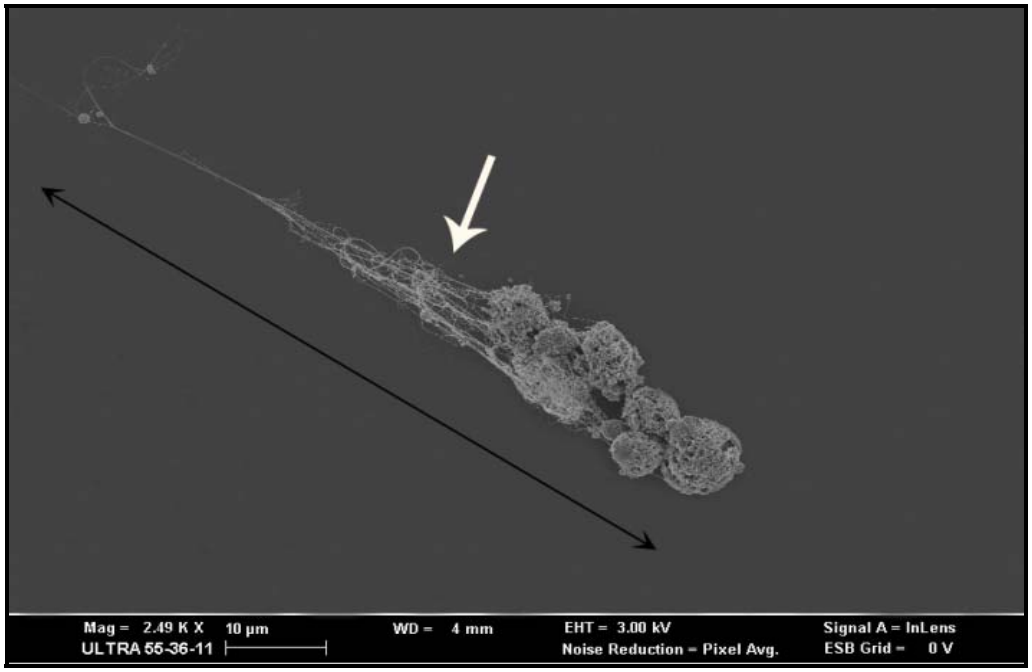

b)

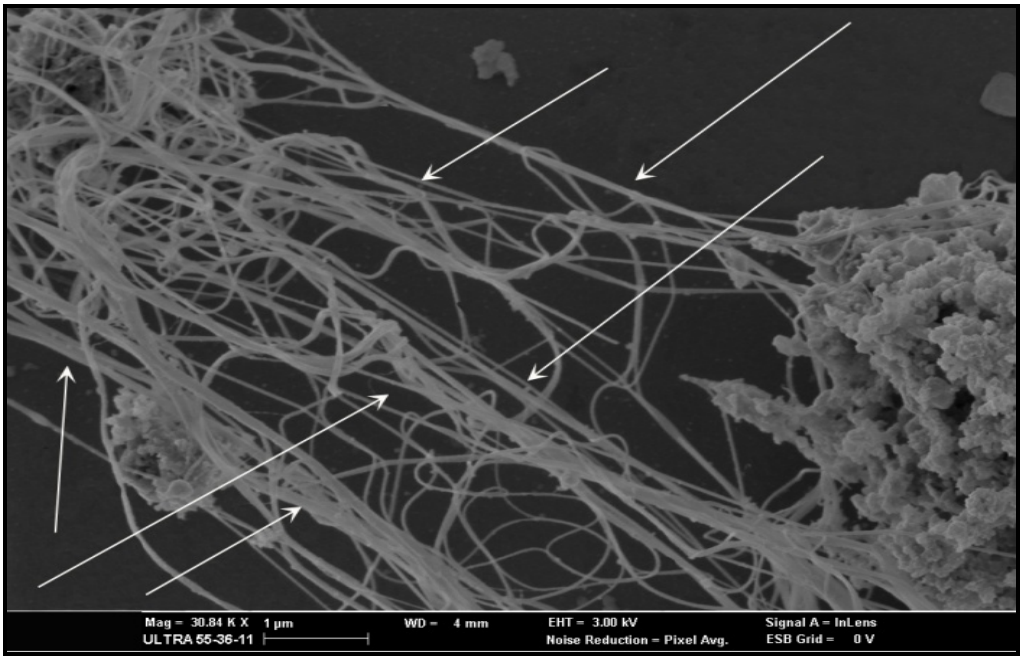

Figure 5.3: Skeletal muscle cells exposed to 0.5% Triton X-100. Complete membrane lyses were seen in these cells. **a**): Low magnification; the thick white arrow indicate the cytoskeleton insoluble to Triton X-100. **b**): Components of the cytoskeleton, thin white arrows indicate microfilaments, intermediate filaments and microtubules.

a)

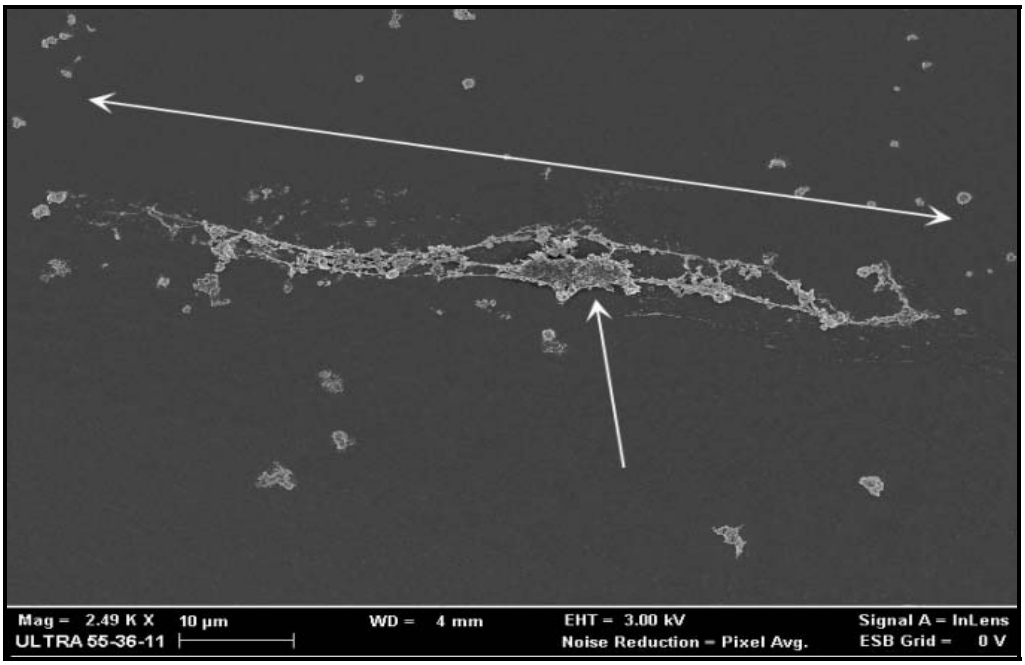

b)

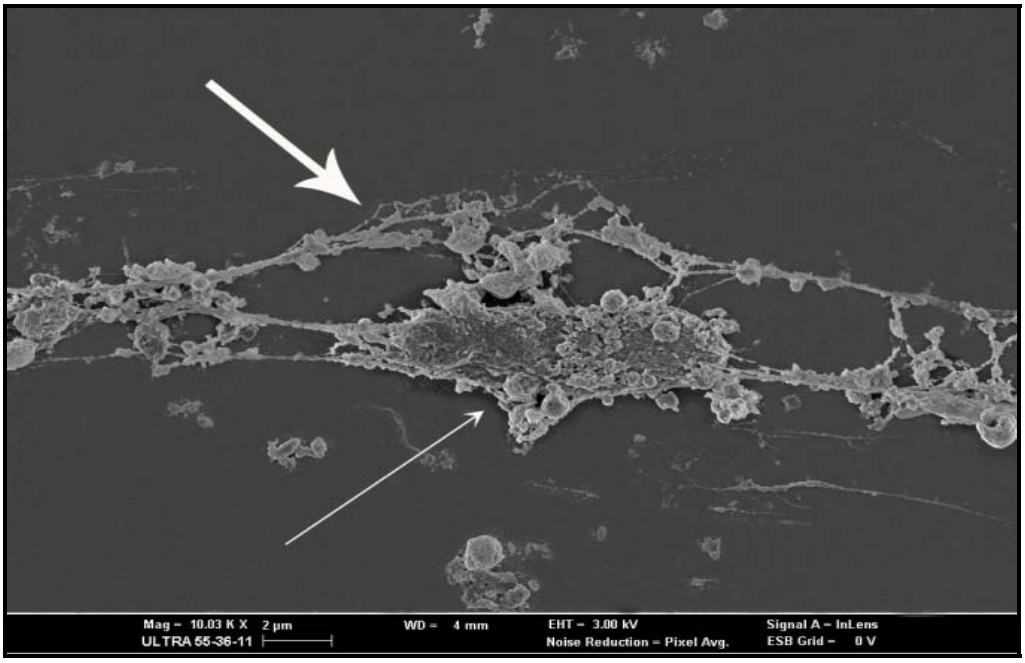

Figure 5.4: Cardiac muscle cells exposed to 0.5% Triton X-100. **a** & **b**): Low and high magnification showing a part of the cytoskeleton (thick arrow in **b**) and the nuclear remnant (thin arrow in **b**), insoluble to Triton X-100 are left.

Wallace *et al*., 1979, demonstrated that, with suitable specimen preparation, it is feasible to resolve and identify the various classes of filamentous structures within a cell or cytoskeleton by SEM, and thus obtain direct three-dimensional information regarding their organization *in situ*. Evidence was presented that cytoskeletal structures (actin filaments, intermediate filaments, and microtubules) in chick embryonic skeletal and cardiac muscle cells can be resolved by SEM after osmium impregnation of biological material, using thiocarbohydrazide as a ligand, followed by critical-point drying (Wallace *et al*., 1979). These different classes of filaments or tubules could be identified both as purified protein polymers and as structured organelles within cryofractured or detergent-extracted cells (Wallace *et al*., 1979). As a prelude to their SEM study of cytoskeletal elements within cryofractured or detergent-extracted cells, it was decided to examine samples of purified F-actin, intermediate filaments (10 nm), and microtubules by negative staining and SEM. When F-actin was deposited on coverslips, processed by the osmium-TCH procedure, and examined at instrumental magnifications of 20 000 – 50 000 by SEM, the filaments exhibited a diameter of 14 - 16 nm, which is approximately twice the width of actin filaments examined by negative stain TEM. The filaments tended to be straight or gently curved, unbranched, and often appear beaded. Polymerized microtubules were also resolved by SEM after the osmium-TCH procedure. The diameter of these structures measured 32 - 37 nm as compared to a diameter of 25 - 28 nm after uranyl acetate negative staining. By SEM, the microtubules exhibited an electron-transparent core, presumably the result of beam penetration through the upper layer of protofilaments. Some microtubules appear rough surfaced but no obvious periodicity had been detected. Intermediate filaments had a complex, branched appearance in which considerable variability of filament diameters were evident. Presumably, this variability reflects extensive side-to-side aggregation of individual filaments. In areas where single filaments were resolved, their diameters measured 10 - 12 nm by negative-stain TEM and 18 - 22 nm by SEM (Wallace *et al*., 1979). In the interior of vertebrate cells, there are dense, heterogeneous and highly interconnected networks; these include the well known structural filaments (microfilaments, intermediate filaments, and microtubules) and the extensive system of highly cross-linked microtrabeculae (Fulton *et al*., 1981). An important aspect of cell structure seen after extraction with Triton X-100 is the surface lamina, an external protein sheet derived from the plasma membrane, which retains the overall morphology and many details of the intact cell. The surface lamina retains most plasma membrane proteins and surface-

specific structures such as binding sites for virusses and lectins (Ben-Ze'ev *et al*., 1979). Fulton *et al*., 1981, suggested that this extracted structure, bound by the protein sheet or lamina formed by the plasma membrane proteins, be designated the "skeletal framework" to distinguish it from the more narrowly defined cytoskeleton.

Severe cellular destruction was seen in both cell cultures upon exposure to the highest concentration of Triton X-100 (0.5%) tested in this study (Figure 5.3 and 5.4). Yu *et al*., 1973 showed that Triton X-100 extraction of cells or membranes solubilizes the bilayer and most integral membrane proteins, leaving only the spectrin matrix and associated proteins in an insoluble, and thus, readily form. The work of Mesher *et al*., 1981, showed that a Triton-insoluble matrix of proteins was associated with the inner face of plasma membranes from murine turmor cells and lymphocytes. The location and properties of the matrix suggested that it might form a membrane skeleton continuous over the inner plasma membrane face of these cells, and consistent with this suggestion, Apgar *et al*., 1985, found that extraction of intact cells (P815 tumour cells) under the same conditions (1% Triton X-100) resulted in structures with a continuous layer of detergent-insoluble protein at the cell periphery. Confined within this peripheral layer was a nuclear remnant (Figure 5.4 b, thin white arrow), the cytoplasmic space was largely empty and clearly lacked filamentous cytoskeletal elements (as seen in Figure 5.3 of this study) (Apgar *et al*., 1985). Low magnification SEM of cardiac and skeletal muscle cells in the present study showed cytoskeletons and cell remnants (Figure 5.3 a & b). Higher magnification showed the complete lyses of membranes (Figure 5.4 a & b), and total loss of cellular integrity, cell cytoskeletons were left without any organelles visible, except for the nucleus, as seen in the cardiac muscle cell in Figure 5.4 b (thin white arrow). Triton X-100 solubilizes membranes of PC12 cells and leaves behind a nucleus and an array of cytoskeletal filaments (as seen in this study in Figure 5.2 b, indicated by thin white arrows) at a concentration of 0.5% (Vale *et al*., 1985). This might be an indication of the presence of proteins in the cytoskeleton that is insoluble to Triton X 100. Biomembranes are not homogenous, they present a lateral segregation of lipids and proteins which leads to the formation of detergent resistant domains, also called "rafts" (Kirat *et al*., 2007), The plasma membrane of cells are composed of the lipid bilayer, integral membrane proteins, and peripheral proteins associated with, but not embedded in, the bilayer (Singer *et al*., 1972 and Bretscher *et al*., 1975). In the erythrocyte membrane, a set of peripheral proteins including spectrin, actin, band 4.1, and ankyrin interact to form

a membrane skeleton associated with the cytoplasmic face of the membrane. This skeleton is a rigid layer that provides mechanical stability to the membrane, plays a role in determining morphology of the cell and appears to influence cell surface protein mobility and lipid distribution in the bilayer (Apgar *et al*., 1985). Fulton *et al*., 1981, showed by direct measurements that most of the surface membrane proteins of prefusion myoblasts and postfusion myotubes remain with the cytoskeletal framework while three-quarters of total cellular proteins are removed (Fulton *et al*., 1981). After mild detergent extraction (0.5% Triton X-100), Prives *et al*., 1982, detected the association of surface acetylcholine receptors with the cytoskeletal framework in cultured muscle cells. The authors found that this procedure distinguished between two subpopulations of this integral membrane protein. The experimental results indicated the following: that i) aggregated acetylcholine receptors were tightly bound to the myotube skeletal framework; ii) a portion of the diffusely distributed acetylcholine receptors were not tightly bound and were extracted with detergent; and iii) the proportion of the tightly bound acetylcholine receptors increased with muscle cell development (Prives *et al*., 1982). Masuko *et al*., 1983, showed with fluorescence microscopy in combination with SEM, that acetylcholine receptor accumulation sites, were associated with smooth surfaced areas of the myotube. The finding was consistent with earlier observations by TEM and freeze-fracture techniques (Masuko *et al*., 1983). Fambrough *et al*., 1978, reported that newly synthesized acetylcholine receptors appeared in the Golgi apparatus and that they may be placed in the membranes of vesicles and subsequently transported to the cell surface by a pathway similar to that taken by secretory proteins. Since areas of acetylcholine receptor clusters in cultured cells represent sites of the most rapid addition of new receptor molecules, rather than of accretion of receptors from surrounding areas of membrane, the smooth surfaced areas corresponding to fluorescent speckles of acetylcholine receptors seem to be areas of insertion of new membranes containing receptor molecules into the sarcolemma.

Many cell types have been shown to contain 3 morphological filament systems: microtubules, intermediate filaments and microfilaments (Goldman *et al*., 1973 and Ishikawa *et al*., 1969). Microfilaments bind heavy meromyosin with the same specificity and morphology as do the thin filaments of muscle and purified filamentous actin (Ishikawa *et al*., 1969 and Huxley, 1963). Microfilaments were therefore considered to be largely composed of actin (Trotter *et al*., 1978). Trotter et al., 1978, used 2% Triton X-

100 to solubilize the membranes of 3T3 cells and extracted the bulk of the cytoplasm, leaving a residue composed of the nucleus and an elaborate system of fibres. Scanning electron microscopy was used to study the distribution of intracytoplasmic fibres. The results of the study argued that the 3-dimensional fibrous network seen in the scanning electron microscope, performs a support function in the cytoplasm, and also plays an important role in cell-substratum adhesion (Trotter *et al*., 1978). The microfilament systems preserved by this method were composed of stereo-chemically intact actin filaments, as shown by their ability to specifically bind heavy meromyosin in characteristic fashion. Intermediate filaments were also retained in the detergent residue, while most microtubules were extracted (Trotter *et al*., 1978).

a)

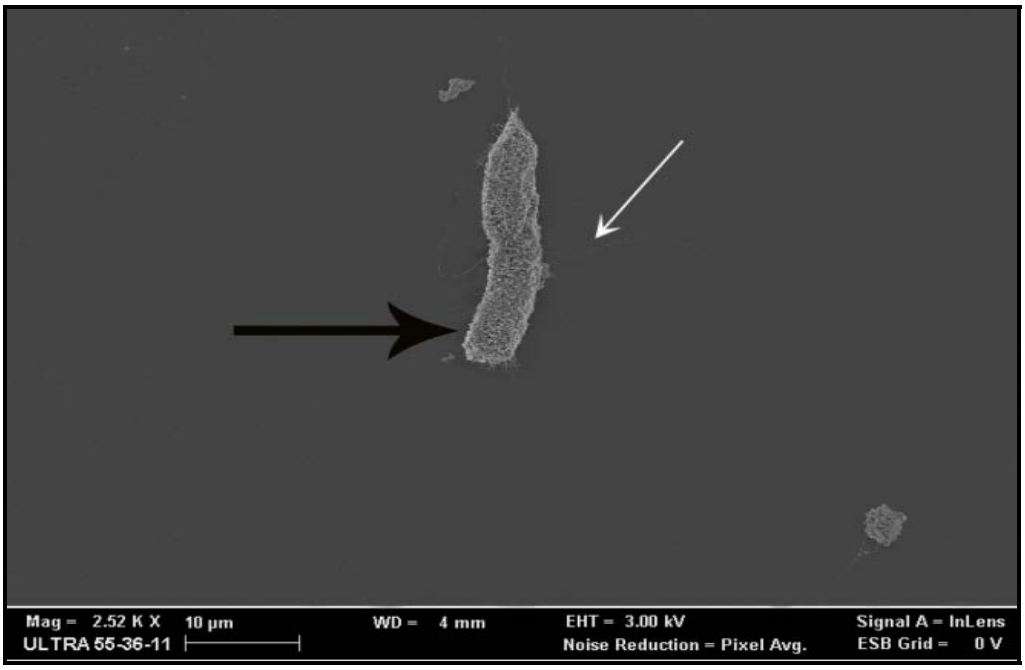

b)

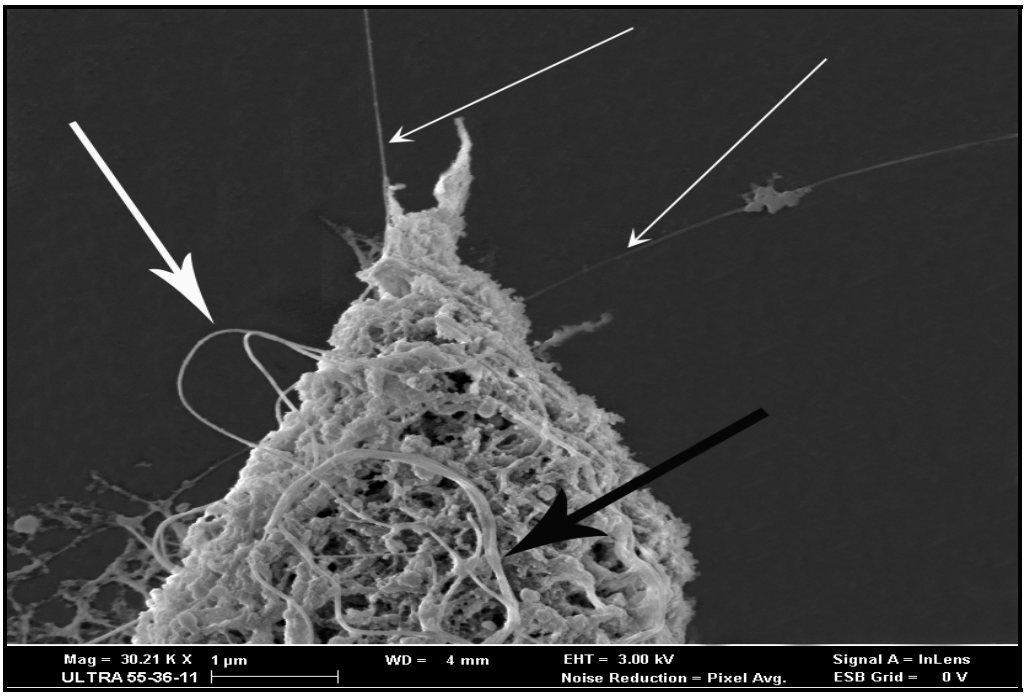

Figure 5.5: Skeletal muscle cells exposed to 0.05% Triton X-100. Low magnification (**a**): showed cell debris and a cell of which the membrane was completely lysed (thick black arrow), with thin filaments extending from the tip of the cell (thin white arrow). **b**): Higher magnification enables visualization of exposed cytoskeletal components. Thin white arrows indicate f-actin filaments, the thick white arrow indicates intermediate filaments, surrounded by vesicular bodies (beaded appearance); the thick black arrow indicates a microtubule (Wallace *et al*., 1979).

a)

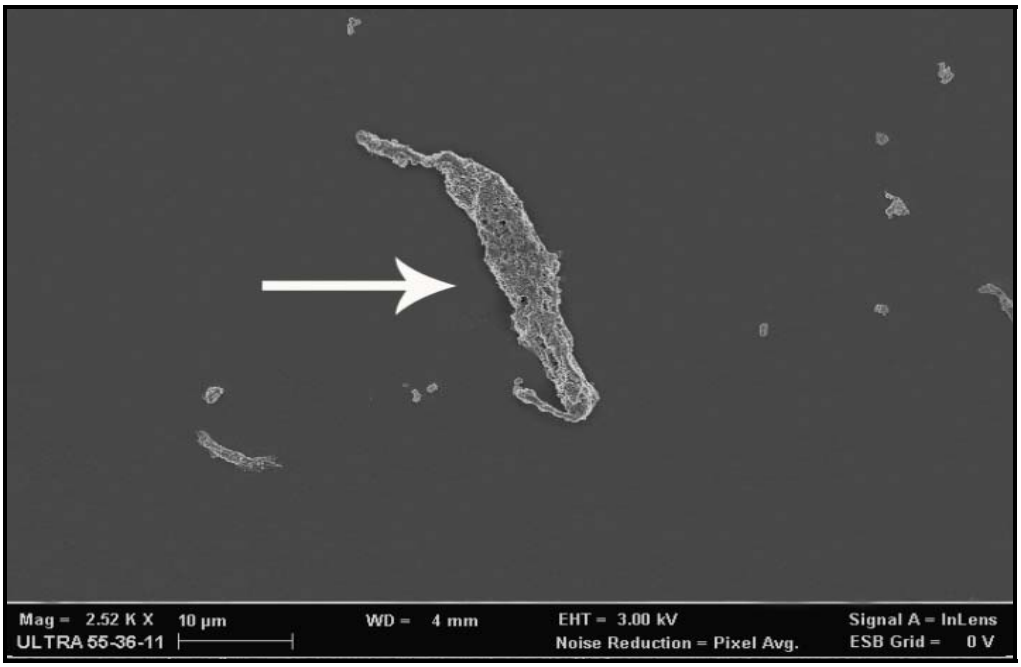

b)

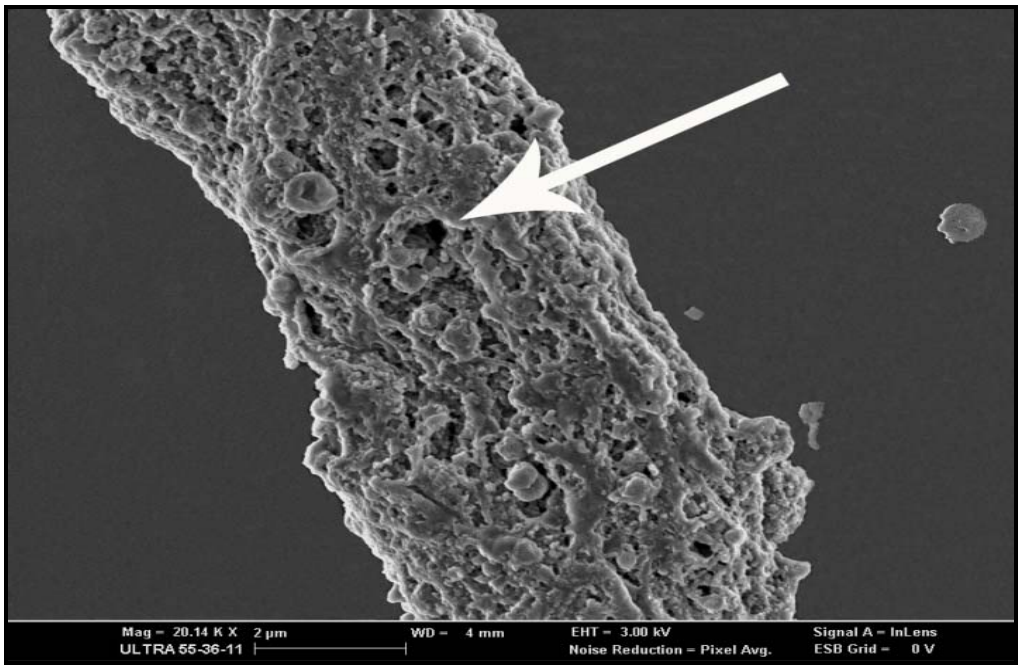

Figure 5.6: Cardiac muscle cells exposed to 0.05% Triton X-100. **a**): At low magnification part of a cell with completely lysed membrane (thick white arrow) and cell debris lying in the vicinity. **b**): At higher magnification, the cell membrane was clearly absent. The thick white arrow indicates what Fulton *et al*., 1981, described as a lacuna. Lacunae in the surface lamina correspond to regions deficient in lectin binding protein, presumably lipid-rich domains in the plasma membrane. The surface proteins form a sheet or lamina that covers the internal skeletal framework remaining after detergent extraction (Ben'Zev *et al*., 1979).

a)

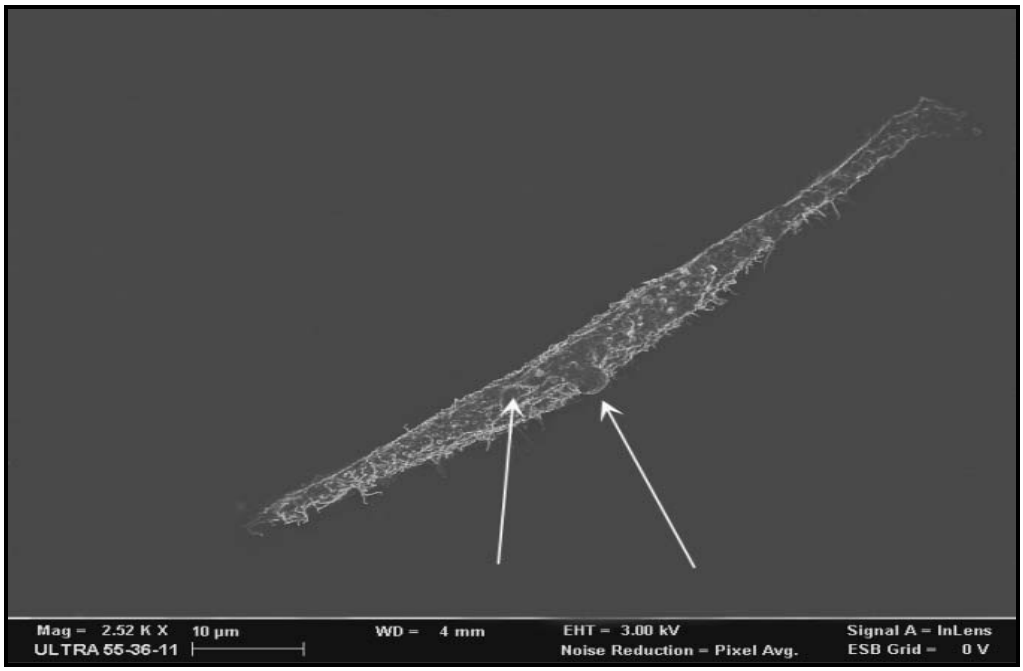

b)

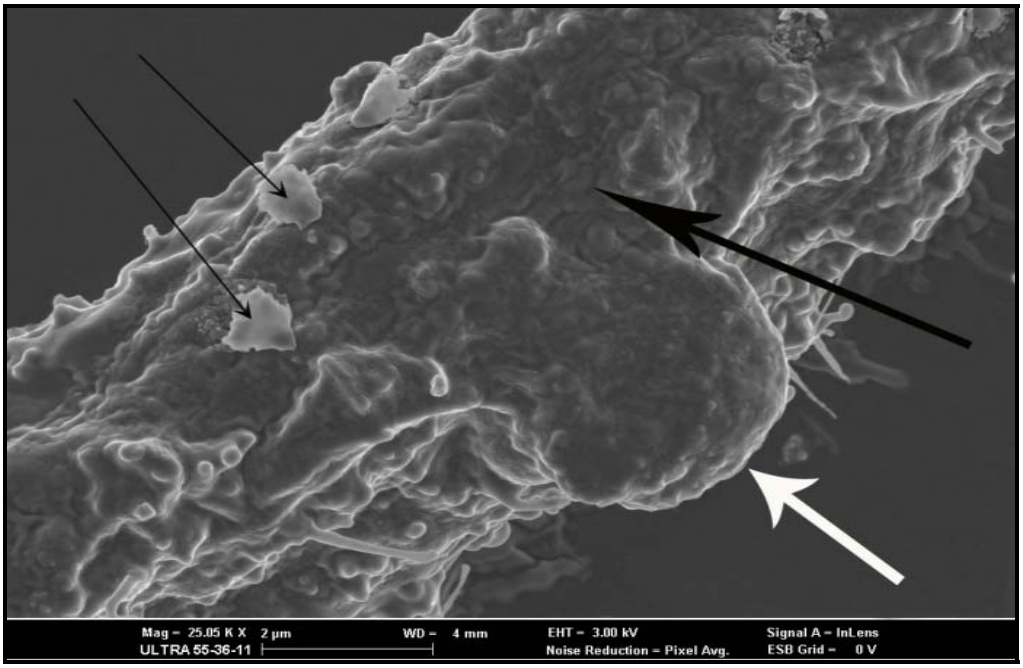

Figure 5.7: Skeletal muscle cells exposed to 0.005% Triton X-100. **a**): At low magnification blebbing was observed on the membrane (thin white arrows). **b**): At higher magnification, it was seen that the membrane was shrunken (thick black arrow). The apoptotic bleb (thick white arrow). Contractile force generated by actin-myosin cytoskeletal structures is thought to drive the formation of membrane blebs and apoptotic bodies (Coleman *et al*., 2001). Ruthenium artefacts (thin black arrows).

a)

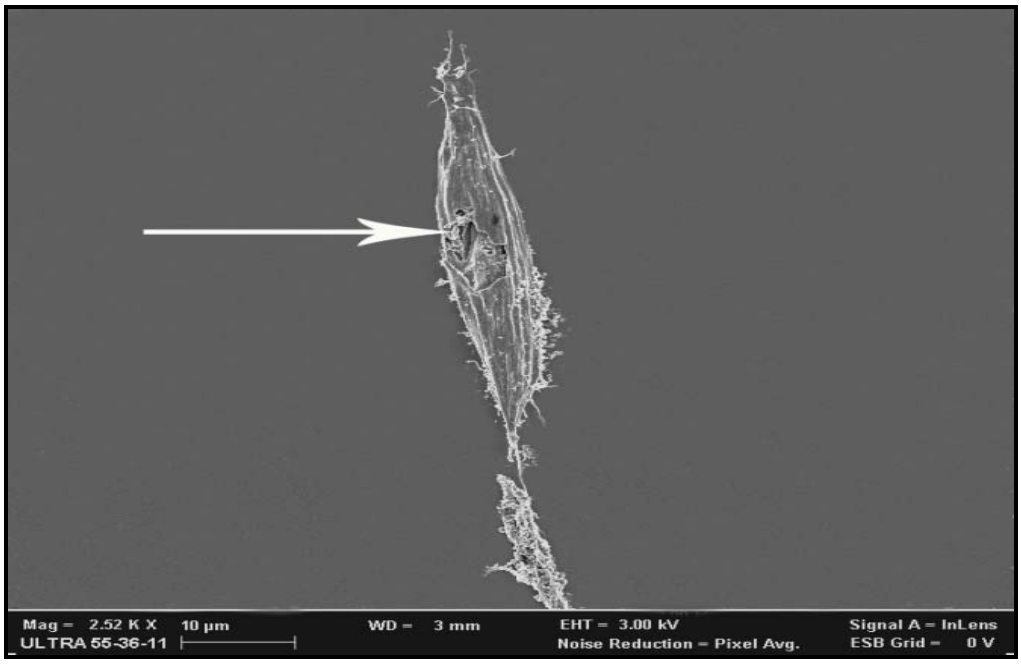

b)

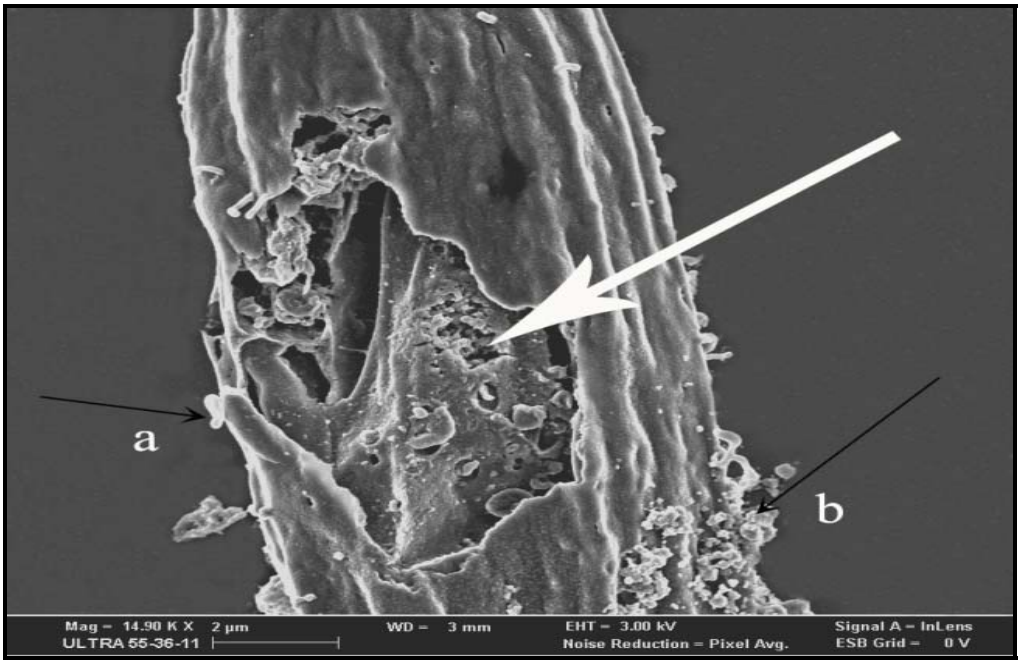

Figure 5.8: Cardiac muscle cells exposed 0.005% to Triton X-100. **a**): Low magnification showed disruption of the membrane (thick white arrow). **b**): At higher magnification it was seen that the membrane collapsed almost in the center of the cell. The surface lamina (thick white arrow) was partly intact, with severe disruptions visible. The thin black arrows show (**a**) a rhutenium artefact; (**b**) protein precipitation, possibly derived from the 5% foetal bovine serum in the culture medium.

The evolutionary conserved execution phase of apoptosis is characterized by events that occur during the final stages of death, including cell contraction, dynamic membrane blebbing and DNA fragmentation (Coleman *et al*., 2001). The distinct morphological transformation is one of the earliest described and most obvious aspects of apoptosis. Contractile force generated by actin-myosin cytoskeletal structures is thought to drive the formation of membrane blebs (as seen in Figure 5.7) and apoptotic bodies (Coleman *et al*., 2001).

It seems likely that the lacunae in the surface lamina relate to the requirements for cell fusion (Fulton *et al*., 1981). Myotube formation requires juxtaposing fusion-competent cell surfaces. The lacunae seen in the postproliferative myoblast in the study by Fulton *et al*., 1981, may reflect an early stage of this process. The act of melding together two surfaces must require unusual membrane properties, perhaps met by the lipid-rich patches characteristic of this stage of muscle development (Fulton *et al*., 1981). Transient lipid-rich patches, relatively free of protein may explain the observation that myoblast lipid fluidity change with fusion (Prives *et al*., 1977). Fulton *et al*., 1981, indicated with fluorescence depolarization measurements a large increase in lipid fluidity just before fusion followed by a decline to normal values after fusion (Fulton *et al*., 1981). Studies by Herman *et al*., 1978, and Kalderon *et al*., 1979, suggested that the lacunae seen in the surface lamina resulted from the protein-free, highly fluid lipid; thus the change in plasma lamina organization may account for the transient increase in lipid fluidity (Fulton *et al*., 1981, Herman *et al*., 1978 and Kalderon *et al*., 1979). The disruption of the membrane surface in Figure 5.8 might be explained by this phenomenon, considering that the concentration of Triton X-100 (0.005%) might be too low to dissolve the membrane proteins, but high enough to disrupt the membrane in protein-free, lipid-rich regions.

a)

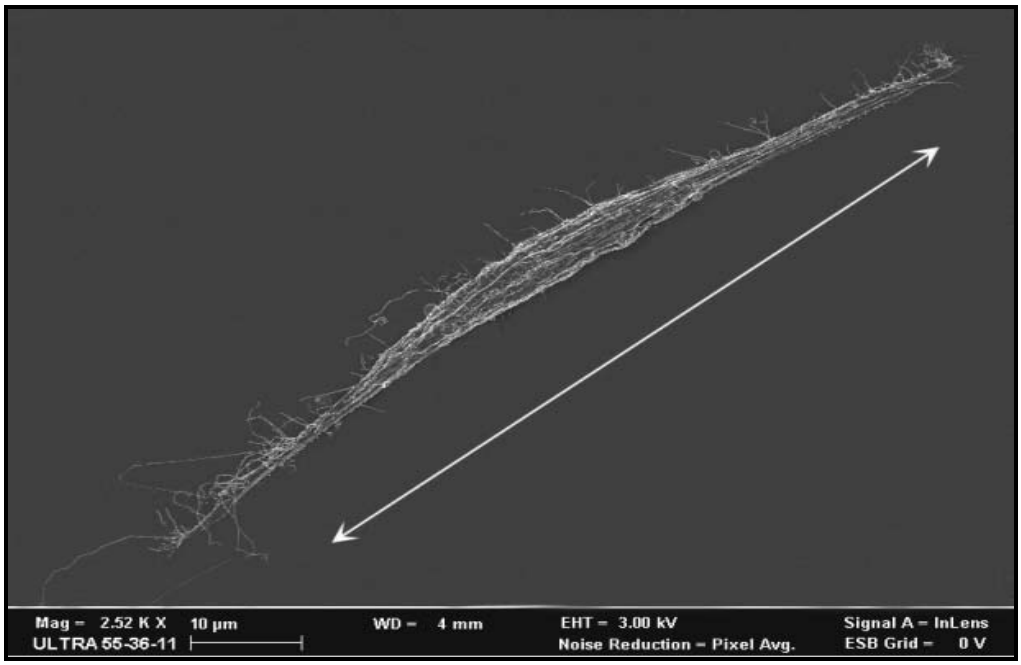

b)

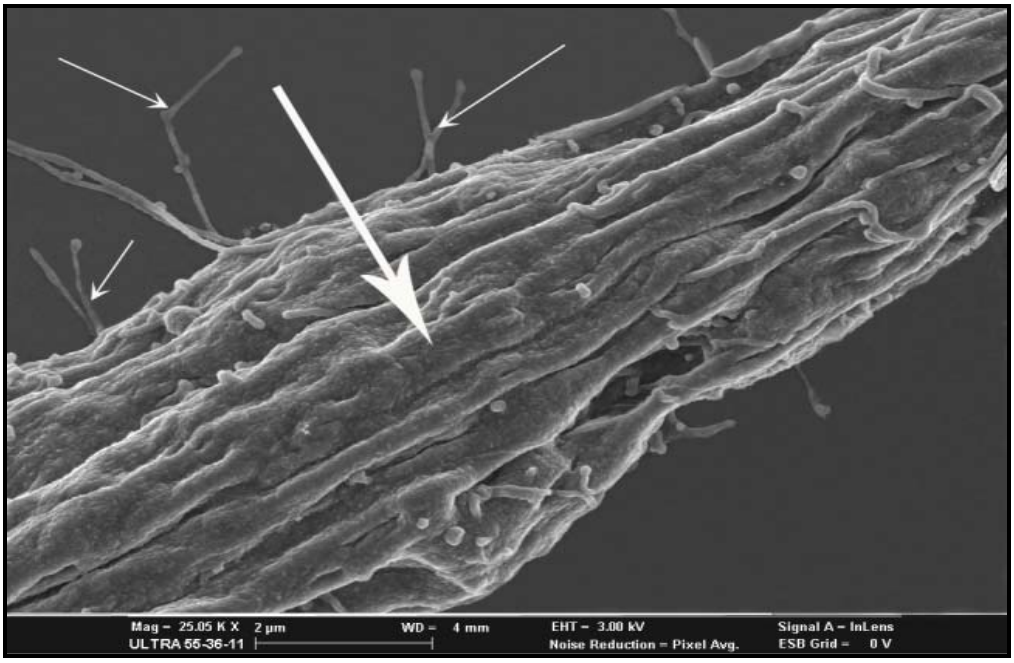

Figure 5.9: Skeletal muscle cells exposed to 0.0005% Triton X-100. **a**): Low magnification shows an intact cell (myoblast) with microprocesses/filopodia extending from the bipolar ends. **b**): At higher magnification it was clear that the membrane was shrunken (thick white arrow) and instable. Microvilli (thin white arrows) extended from the membrane, which might be a possible indication of the cell's state in the cell cycle (Late G_2, Masuko *et al*., 1983). Although no myotubes or fusion of myoblasts were observed at this concentration, the myoblast (**a**) might be in proliferating state.

a)

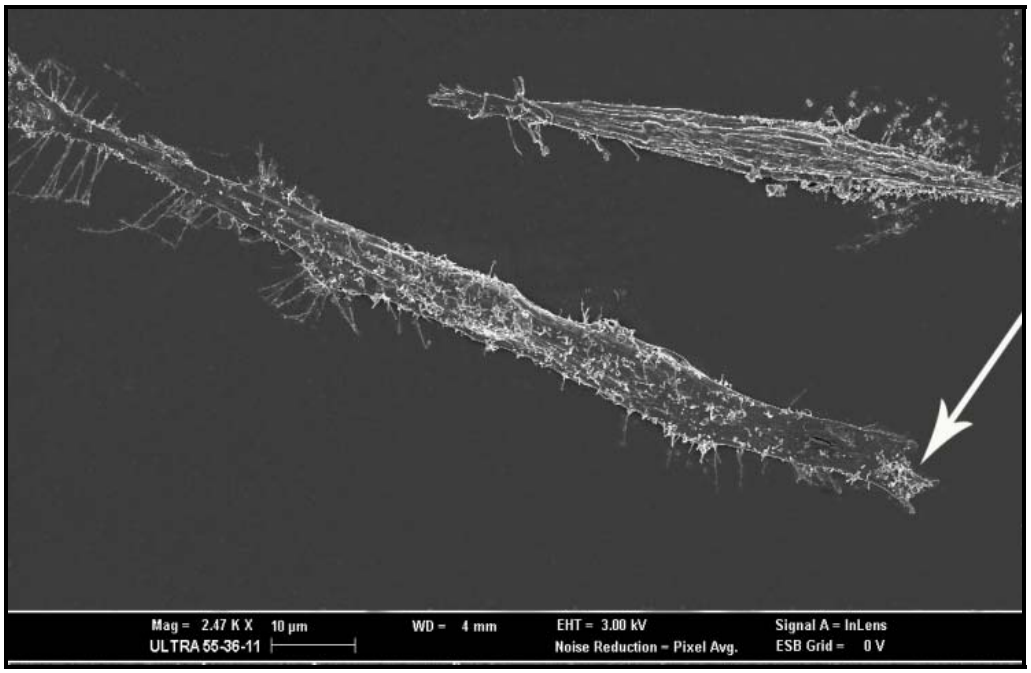

b)

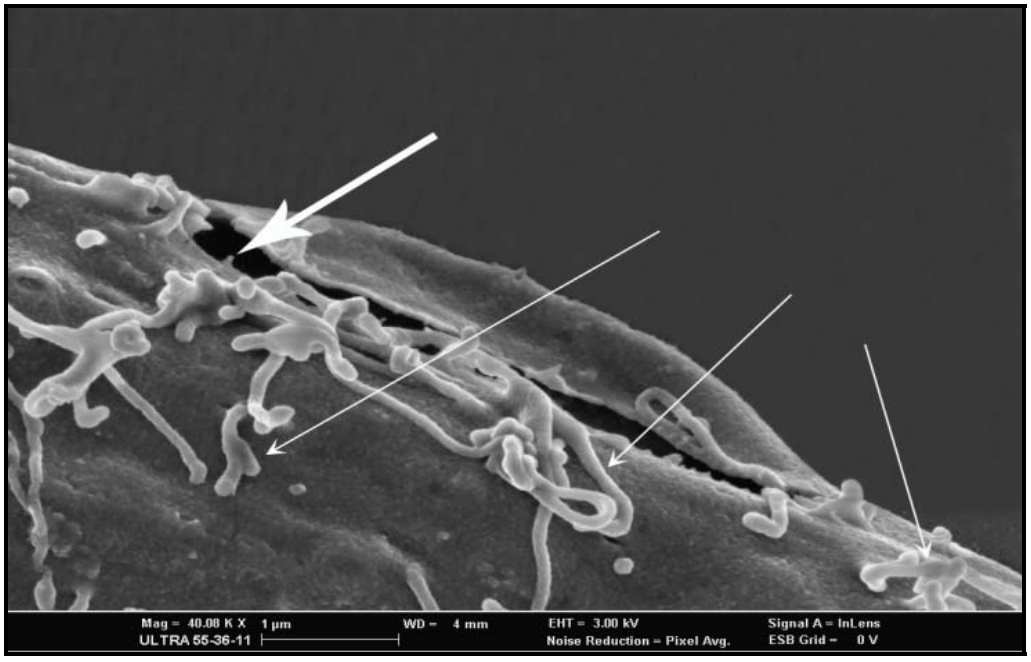

Figure 5.10: Cardiac muscle cells exposed to 0.0005% Triton X-100. **a**): Low magnification shows two intact cells (myoblasts) with bipolar ends with extending microprocesses/filopodia possibly in proliferating state. The thick white arrow indicates the very characteristic end of a cardiac cell. **b**): higher magnification showed a smooth membrane surface, possibly unstable (thick white arrow indicate a tear in the membrane), thin white arrows indicate microvilli confirming the state of proliferation.

a)

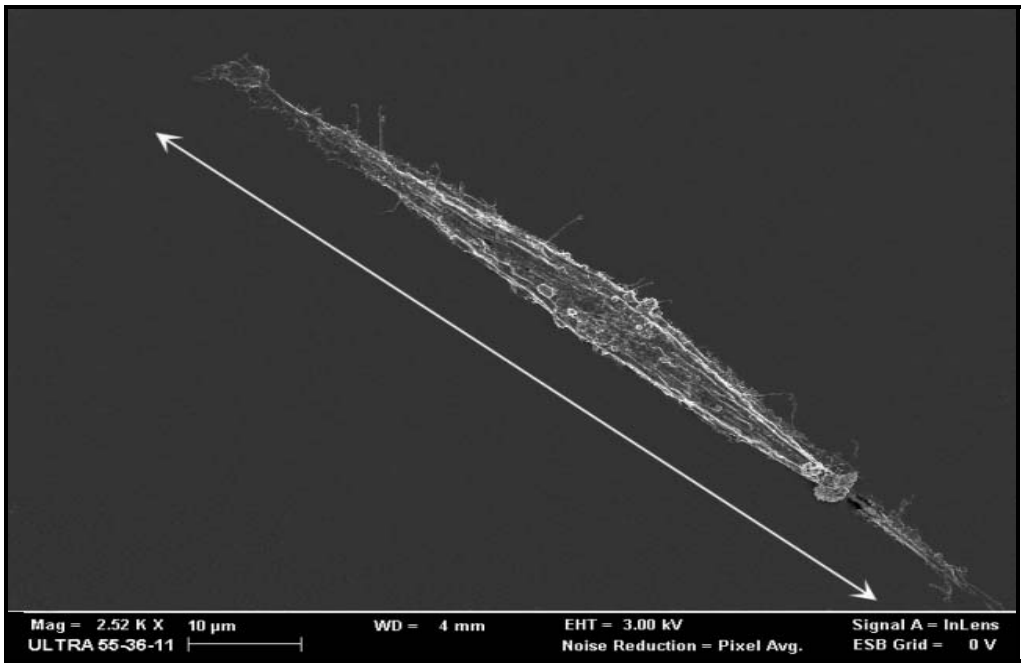

b)

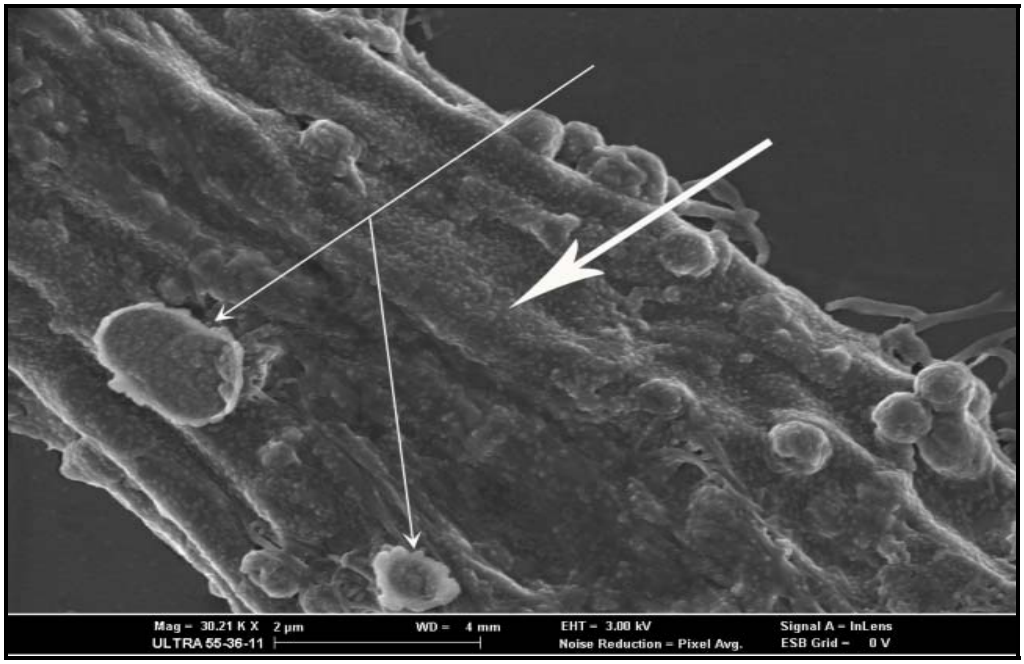

Figure 5.11: Skeletal muscle cells exposed to 0.00005% Triton X-100. **a**): Low magnification shows bipolar ends with extending microprocesses. **b**): Higher magnification shows that the membrane is not smooth, it almost appear to have a rough surface (thick white arrow). Thin white arrows indicate ruthenium artefacts.

a)

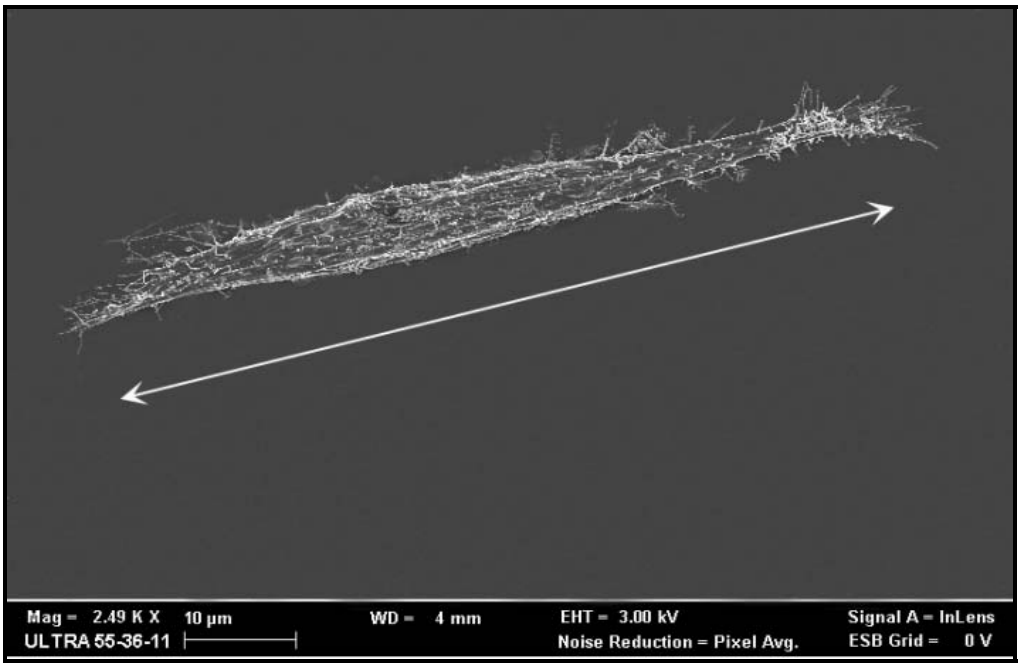

b)

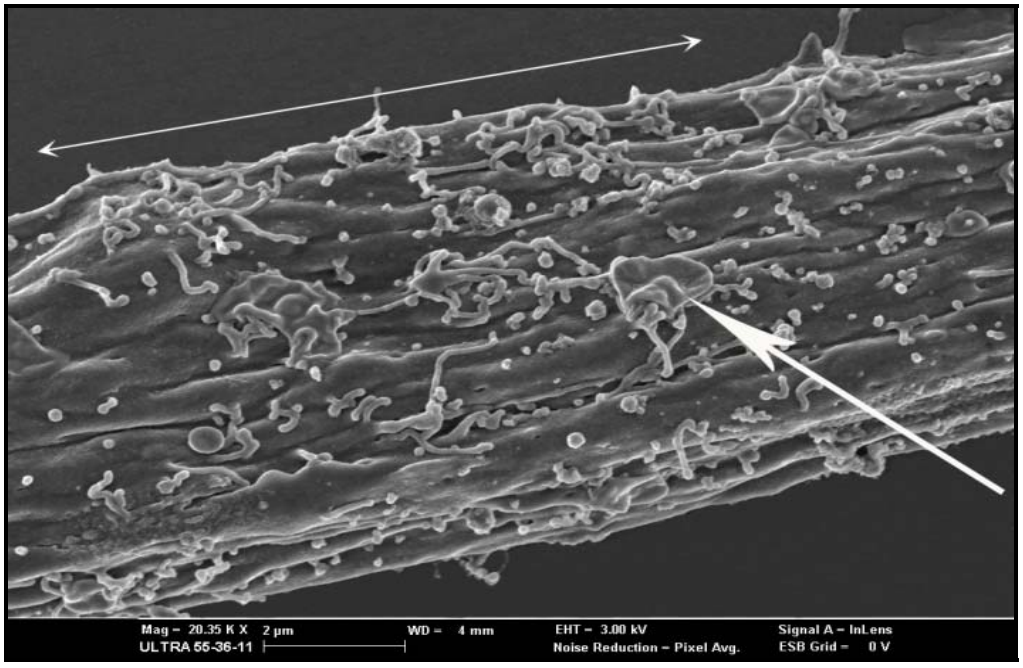

Figure 5.12: Cardiac muscle cells exposed to 0.00005% Triton X-100. **a**): Low magnification shows a bipolar intact cell with extending microprocesses. **b**): On higher magnification the membrane show shrinkage with numerous microvilli, possibly the cell is in proliferating state. Thick white arrow point to an artefact lying on the membrane surface.

5.3.3 Cells Exposed to CoQ10

a)

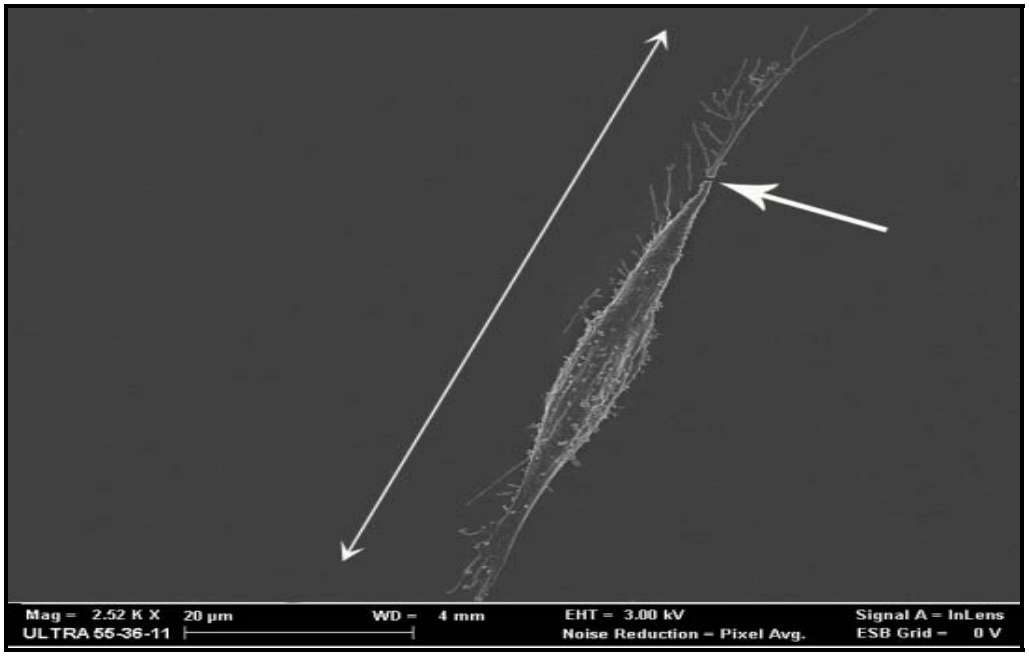

b)

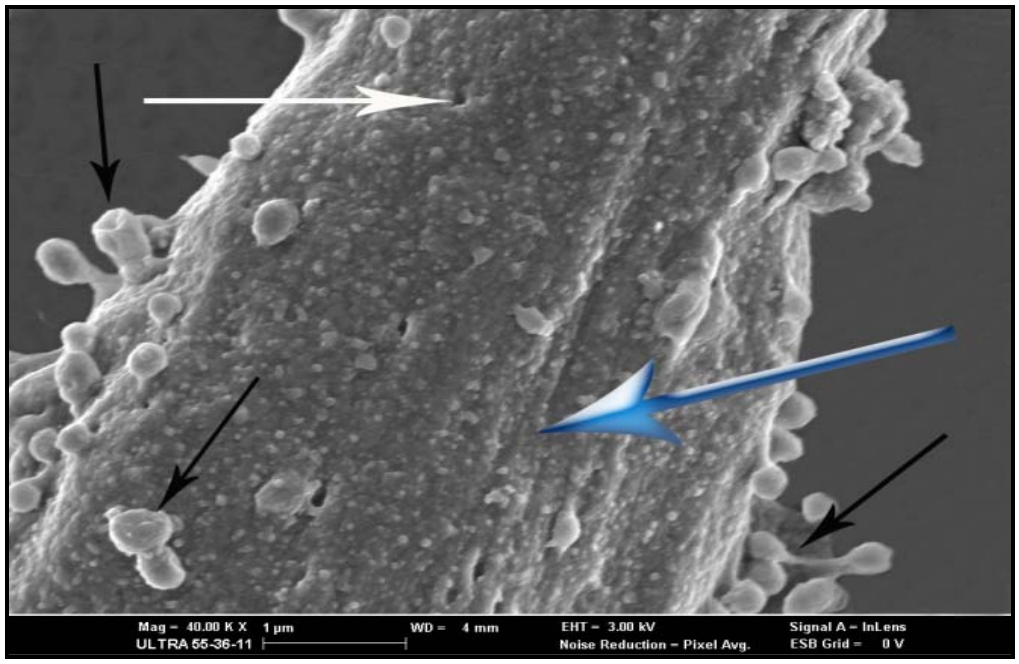

Figure 5.13: Skeletal muscle cells exposed to 0.2mg/ml CoQ10. **a**): Low magnification shows an intact spindle-shaped cell with bipolar ends and microprocesses (thick white arrow indicate breakage of the upper tip of the cell, which might be due to critical point drying. **b**): Higher magnification shows an intact membrane (blue arrow), the surface seems rough with numerous mcirovilli (thin black arrows) and small spherical protrusions starting to protrude from the membrane. The thick white arrow indicates an ion channel in the membrane.

a)

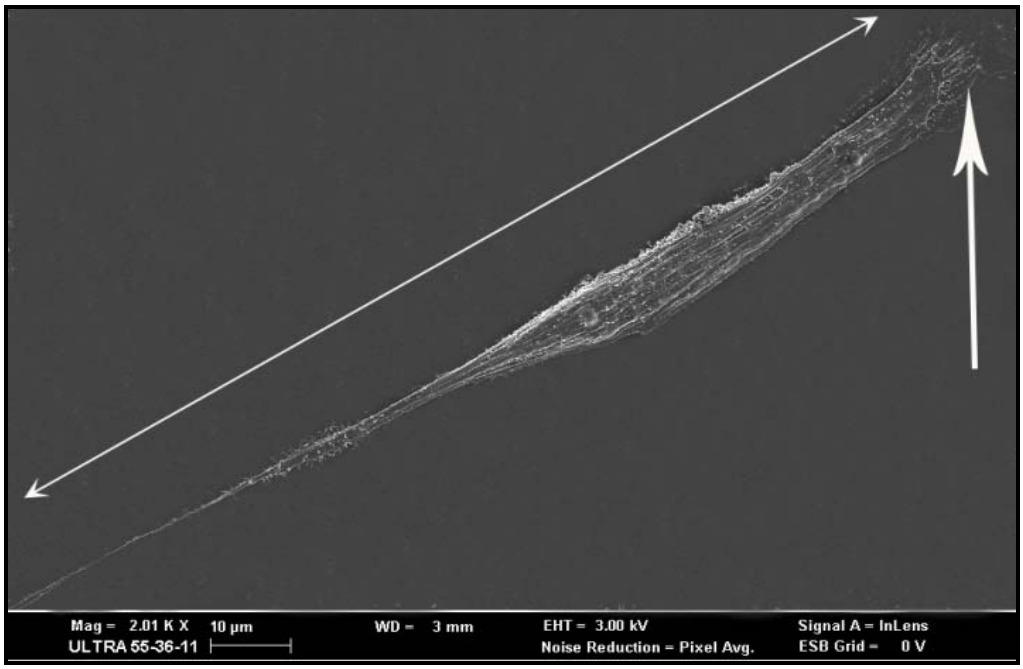

b)

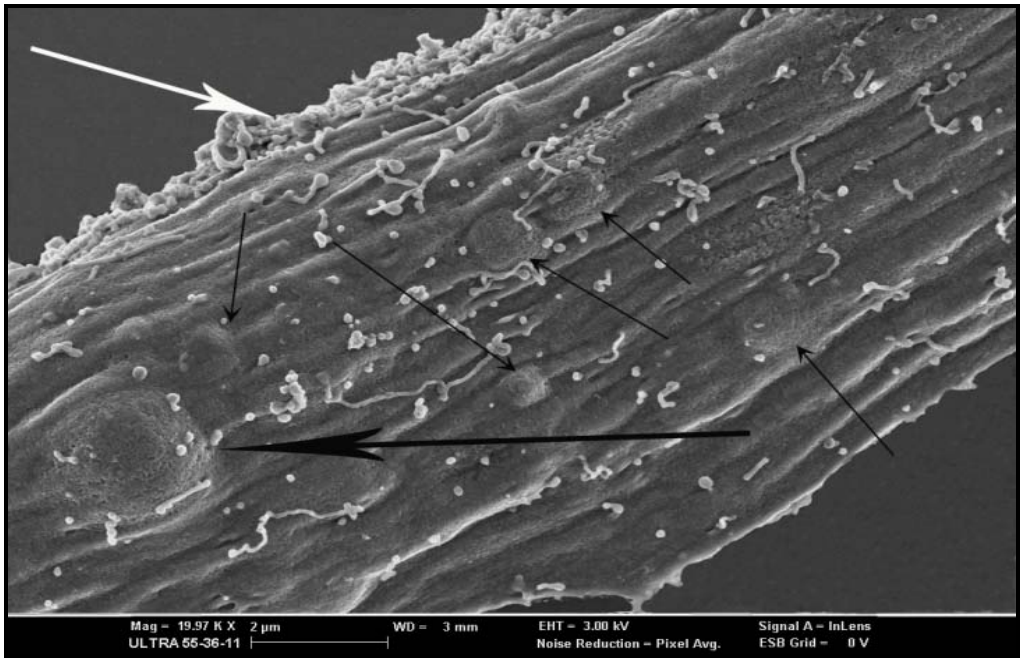

Figure 5.14: Cardiac muscle cells exposed to 0.2mg/ml CoQ10. **a**): Low magnification possibly shows a myoblast entering fusion. Broad flat upper end with numerous extending microprocesses, numerous microvilli, small spherical protrusions (**b**: thick white arrow), and a bulging appearance (**b**: thick and thin black arrows), indicating that the cell are possibly in the M phase of the cell cycle. **b**): The membrane is largely intact with a few slightly rough patches.

a)

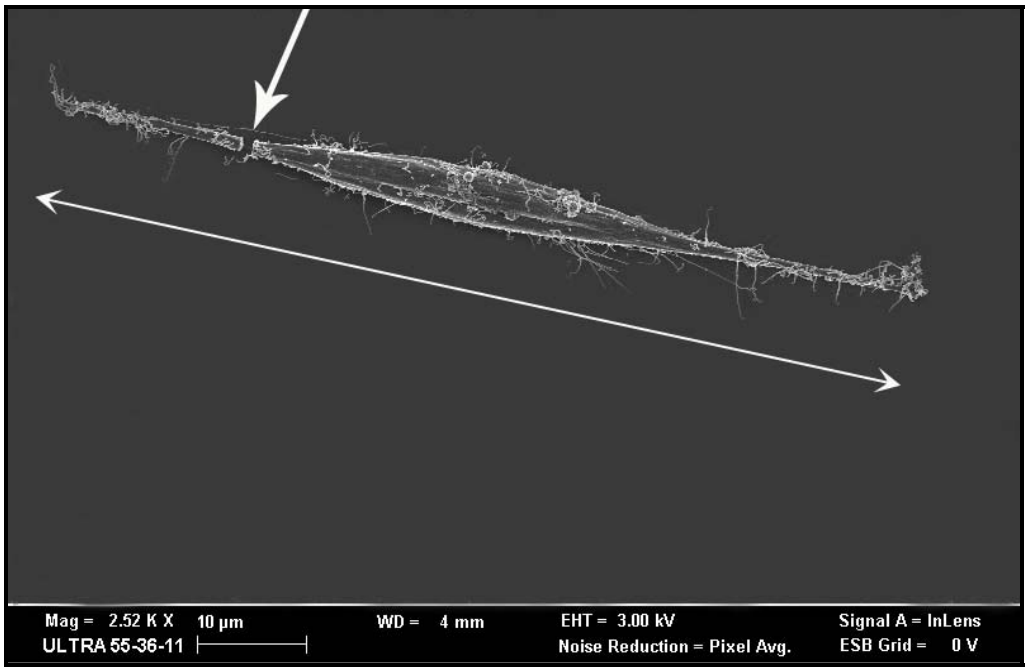

b)

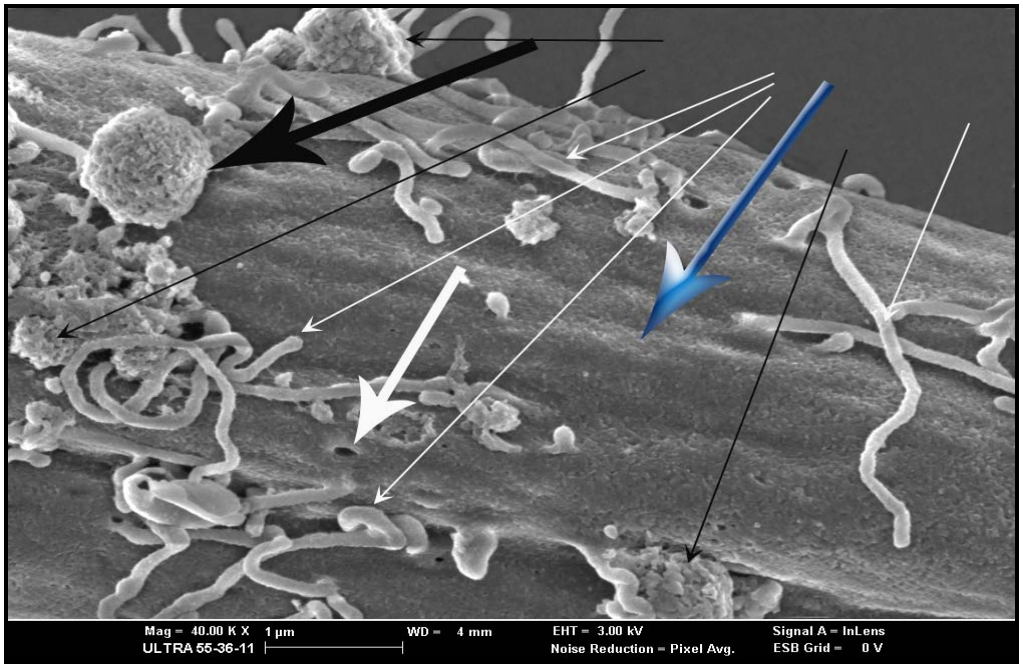

Figure 5.15: Skeletal muscle cells exposed to 0.1mg/ml CoQ10. **a**): Low magnification shows an intact skeletal muscle cell with extending microprocesses. Breakage of the tip is probably due to critical point drying procedure (thick white arrow). **b**): High magnification shows and intact membrane (blue arrow), microvilli (thin white arrows). Ion channels are visible (thick white arrow). Protein precipitation occurred due to proteins present in culture medium (black arrows).

a)

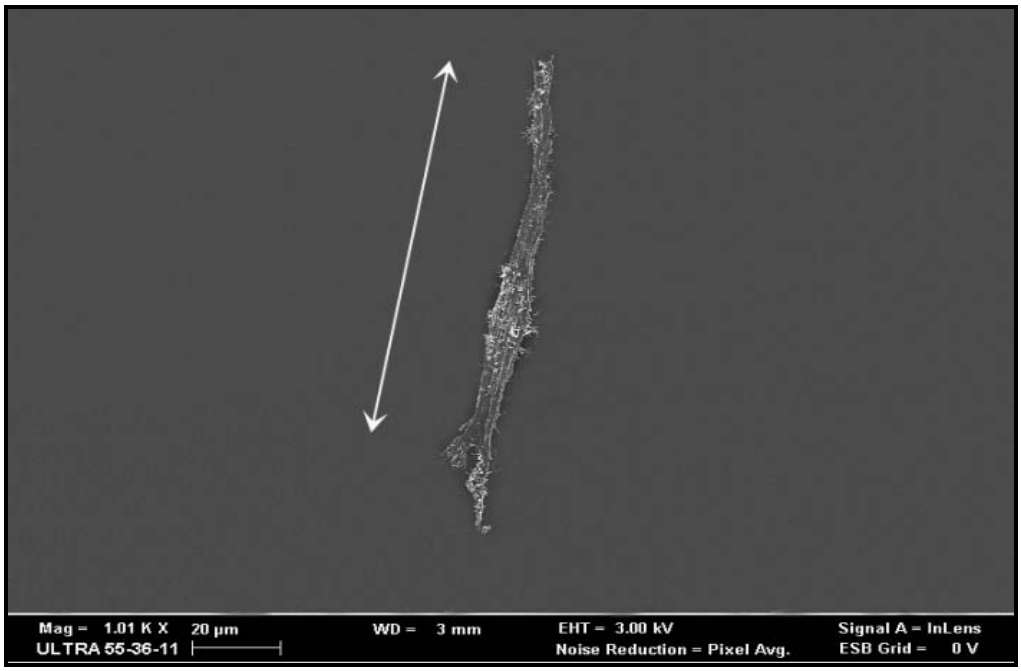

b)

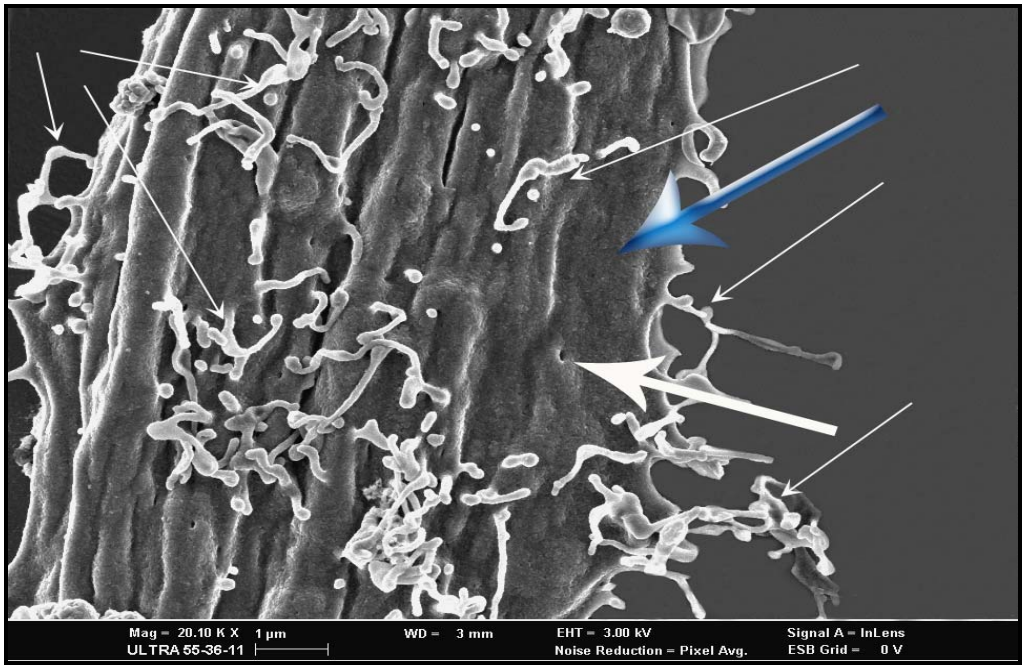

Figure 5.16: Cardiac muscle cells exposed to 0.1mg/ml CoQ10. **b**): High magnification shows numerous microvilli (thin white arrows), although the membrane presented with a slight shrunken appearance, it was intact (blue arrow). Ion channels are visible (thick white arrow).

a)

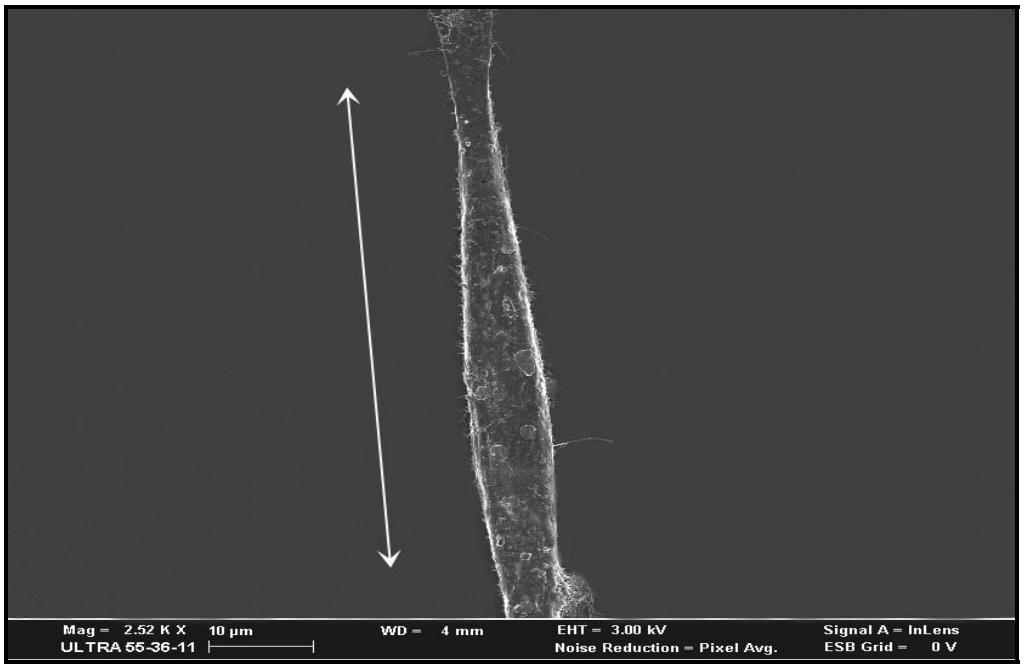

b)

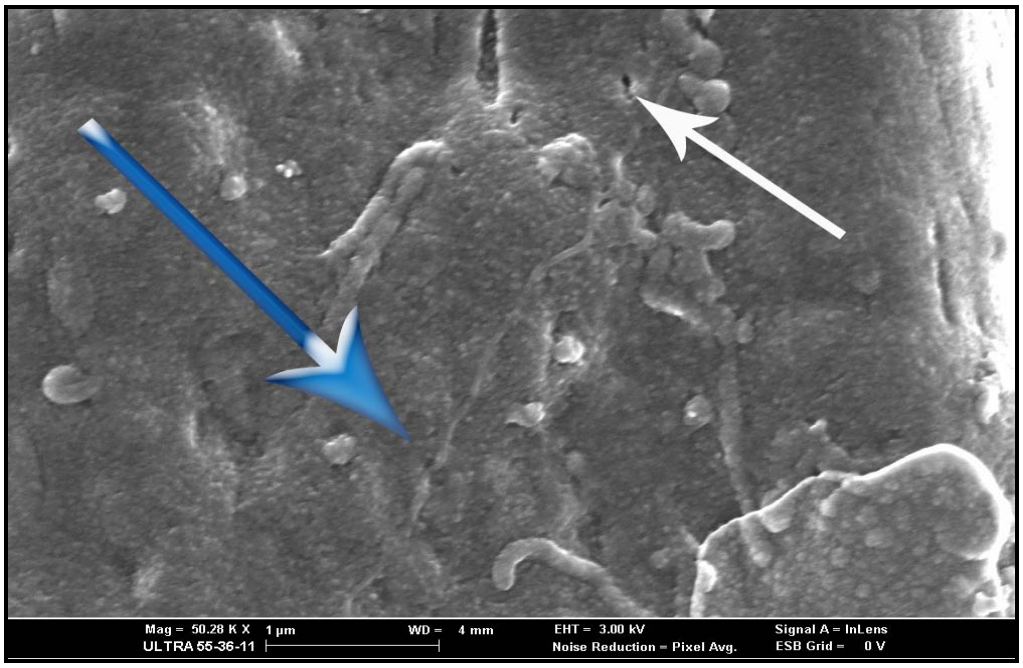

Figure 5.17: Skeletal muscle cells exposed to 0.05mg/ml CoQ10. **a**): Low magnification shows a cell which is possibly postproliferative (myotube), when considering the size. The relatively smooth cell surface seen at higher magnification (**b**), is characteristic of cells capable of undergoing fusion, probably in the G_1 phase of the cell cycle (Masuko *et al*., 1983). The membrane was perfectly intact (blue arrow). Ion channels are visible (white arrow).

a)

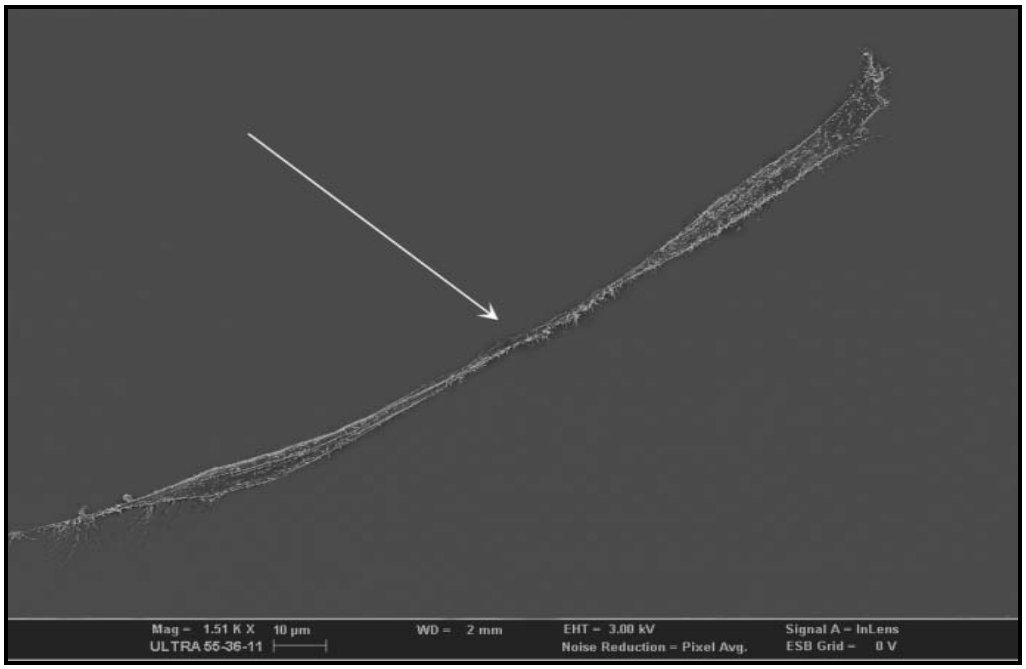

b)

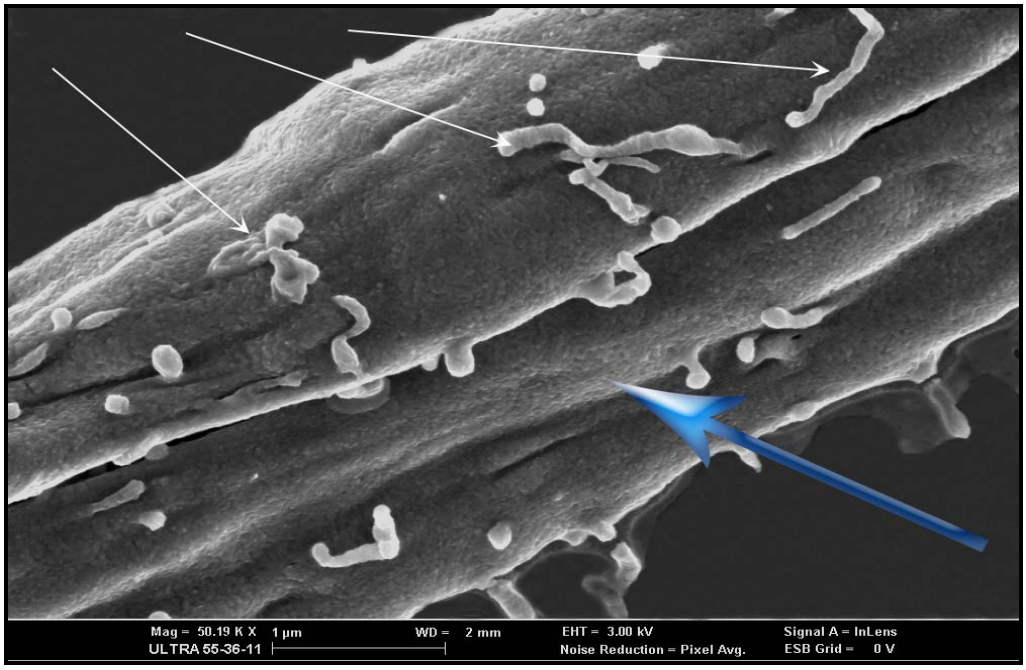

Figure 5.18: Cardiac muscle cells exposed to 0.05mg/ml CoQ10. **a**): Low magnification shows two myoblasts after fusion, forming a myotube. **b**): High magnification shows a smooth, intact membrane (blue arrow), microvilli and small spherical protrusions are present (thin white arrows), characteristic of the surface structure of newly formed myotubes.

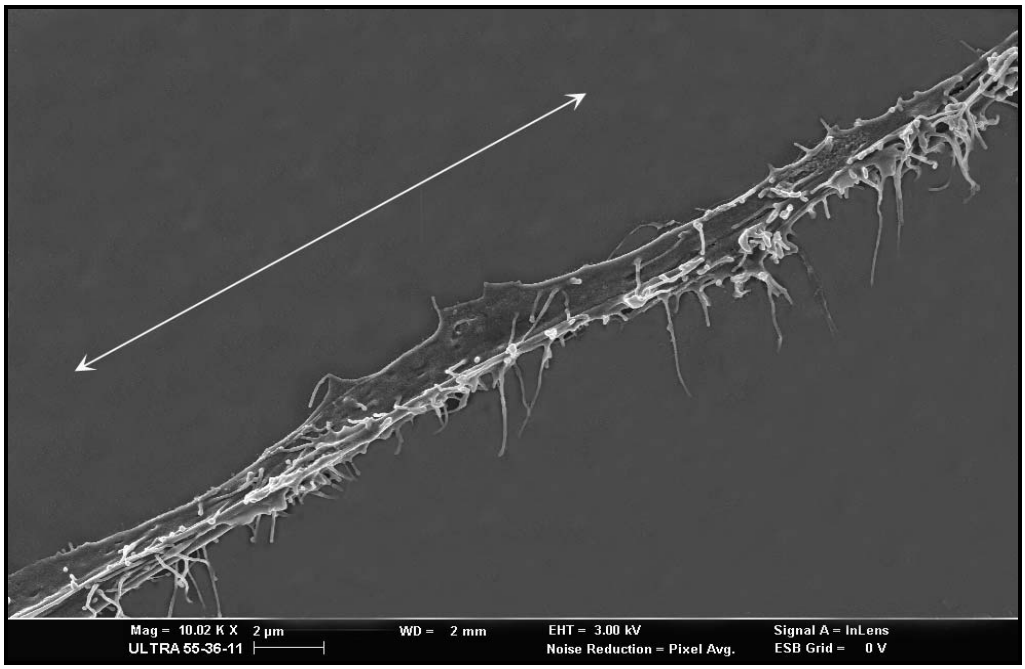

Figure 5.19: The arrow showed the area where the two myoblasts in Figure 5.17 **a**, has fused to form a myotube. The establishment of this connection generate considerable tension indicating that possibly these cells are drawn together (Singer *et al*., 1984).

The formation of muscle fibres by myoblasts fusing is a striking example of the skeletal framework (described by Fulton *et al*., 1981) reorganizing during development (Fulton *et al*., 1981). During differentiation, the structural aspect of the cell becomes reorganized from a diffuse network of filaments in pre-myoblast cell into linear, axially orientated filament bundles characteristic of myoblasts fusing together (Pudney *et al*.,1980). Myoblasts fuse to form multinucleated myotubes which then synthesize and organize the banded actomyosin contractile apparatus. Cells develop under optimum *in vitro* conditions to mature, twitching muscle fibers. Both the internal networks and surface lamina in the myoblast undergo profound, concurrent, yet distinct changes in preparation for and after fusion (Fulton *et al*., 1981). To form the multinucleated myotube, plasma membranes of fusion–competent myoblasts must meld; at this time, large openings, or lacunae, in the surface lamina appear. The work of Huang *et al*., 1978, indicated that prior to the formation of the myotube, long actin-rich processes, “microprocesses”, were extended from myoblasts, sometimes over a distance of 200µm. These long cytoplasmic microprocesses (0.1µm in diameter) exhibit splayed ends resulting from the unravelling

of the microfilament, reminiscent of the “growth cone” of axons (Yamada *et al*., 1971), and is a characteristic of cultured differentiating chick muscle cells (Singer *et al*., 1984). When these processes contacted each other, they fuse prior to the union of the respective cell bodies; then undergo a complex realignment which seemingly reorientates both microprocesses into a single filament bundle, resulting in generation of considerable tension indicating that these cells are actively drawn together (Singer *et al*., 1984). The junction formed between two myoblasts (Figure 5.17 & 5.18) at fusion then disappears and the internal structural networks reorganize to form a continuous structure oriented along the muscle fibre axis (Fulton *et al*., 1981). Myoblasts that are still proliferating also form an almost continuous surface lamina. These proliferating myoblasts are typically short, bipolar cells with ruffled or knobbed tips (Figure 5.13 & 5.15). When cells prepare to fuse, they have a sparse skeletal structure, lightly cross-linked and nearly empty, with a few major filamentous cables that terminate the cell periphery. The morphology and surface lamina of postproliferative myoblasts show marked specialization, as they take on a new morphology as they prepare to fuse and form multinucleated myotubes, becoming elongated and more spindle-like. One or both tips have a complex ruffled and knobbed configuration; the other end may be pointed. The remainder of the plasma membrane appears relatively smooth (Fulton *et al*,. 1981).

Fulton *et al*., 1981, investigated myoblasts from 12 day chick embryo breast muscle. Upon detergent extraction, many large opening or lacunae were seen in the surface lamina of the postproliferative myoblast. The extremities of the postproliferative myoblast framework have largely collapsed and the surface lamina in these regions has a very discontinuous, reticulate appearance. An extracted tip showed the typical fibrillar substructure underlying the lacunae, prominent fibrous structures were seen where the surface lamina was absent. The lacunae in the surface lamina of the postproliferative myoblasts were very likely related to the formation of cell-to-cell junctions during fusion and were found principally in regions where junction formation was expected. The lacunae in postproliferative myoblasts disappear quickly after fusion and the lamina becomes almost entirely continuous. Because the surface lamina is formed by plasma membrane proteins, these lacunae indicated that myoblasts organize plasma membrane proteins in an exceptional and characteristic way. Fulton *et al*., 1981, showed that these lacunae were not formed by extensive loss of surface protein, and suggested that the

lacunae in the surface lamina corresponded to regions deficient in lectin binding protein that are presumably lipid-rich domains in the plasma membrane.

Changes in surface morphology were observed in newly formed chick myotubes by Masuko *et al*., 1983. The surface over the nucleus is smooth whereas the surface in perinuclear regions has become broad flat excrescences, microvilli, and small spherical protrusions. These surface features become less prominent as the myotubes mature, and spherical protrusions and microvilli are widely distributed on the cell surface of striated myotubes (Masuko *et al*., 1983). Myoblasts arrested at fusion in the study by Masuko *et al*., 1983, had a relatively smooth surface resembling that of cells in the G_1 phase of the cell cycle. Since myogenic cell fusion occurs during the G_1 phase of the cell cycle (Okazaki *et al*., 1966 and O'Neill *et al*., 1972), this relatively smooth surface may be characteristic of cells capable of undergoing fusion that have not yet entered the fusion process (Masuko et *al*,. 1983). Huang *et al*., 1978 found that calcium-deficient medium (160μM) inhibits fusion of chick myoblasts from chick embryonic breast muscle cells. Subsequent to the addition of the medium, they found that the deficiency in calcium augments the proportion of long processes in the culture and inhibits the pulling together of the cells, thus making it difficult to draw conclusions on the state of fusion.

Ion channels are proteins, forming transmembrane pores in biological cell membranes. Opening and closing of the pores regulate the ion currents through the membrane, and consequently vital bodily functions from hormonal homeostasis to cognition (Elinder *et al*., 2007). The ubiquitous presence of ion channels among cells of unicellular and multicellular organisms suggests their importance in maintaining cellular integrity (Laniado *et al*., 1997). Ion channels are classified broadly by the principal ion they carry (Sodium, Potassium, Calcium, Chloride) and the mechanisms by which they are opened and closed. Changes in membrane voltage or concentrations of intracellular ions and molecules such as calcium and ATP can also open ion channels (Laniado *et al*., 1997). Stimuli activating channels are multifarious; channels are opened chemically by ligands such as neurotransmitters, calcium ions, and cAMP; mechanically by stretching the membrane; or electrically by changing the transmembrane voltage. The detailed molecular mechanisms of these opening processes are poorly understood (Elinder *et al*., 2007).

The membrane stabilizing property of CoQ10 has been postulated to involve the phospholipid-protein interaction that increases prostaglandin (especially prostacyclin) metabolism. It is thought that CoQ10 stabilizes myocardial calcium-dependent ion channels and prevents the depletion of metabolites essential for ATP synthesis (Shinde *et al*., 2005). It has also been shown to help preserve myocardial sodium-potassium adenosine triphosphatase activity and stabilize myocardial calcium-dependent ion channels (Terao *et al*., 2006). The results of a study by Okamoto *et al*., 1995, suggested that one of the causal mechanisms of muscular injury is an increase in calcium concentration, due to the excess entry of extracellular calcium, and that CoQ10 can protect skeletal muscle cells against such undesirable biochemical changes (Okamoto *et al*., 1995). Crane, 2001, reported the participation of the quinine in oxidation of thiol groups on growth factor receptors or membrane ion channels, and gave the example of ryanodine receptors, controlled by calcium release which may also be related to oxygen sensing (Crane, 2001). Crane, 2001, also indicated the role of Coenzyme Q in proton movement, indicated at the plasma membrane. In this situation Coenzyme Q is involved in activation of Na^+/H^+ exchange across the membrane carried out by the Na^+/H^+ antiport. The energy for this process is based on a high concentration of Na^+ outside the cell which exchanges for protons in the cell. The Na^+ is then pumped out of the cell by the Na^+/K^+ ATPase which obtain energy from ATP. During this ATP action excess Na^+ is released so the cell develops an inside negative membrane potential which is important for many cellular functions and transport action (Crane, 2001).

a)

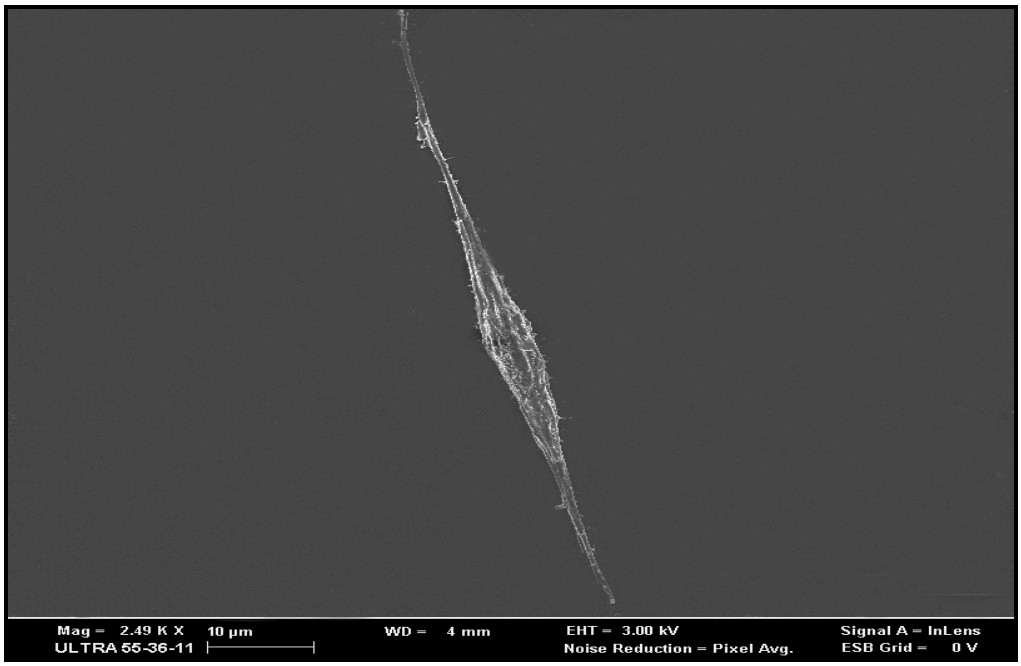

b)

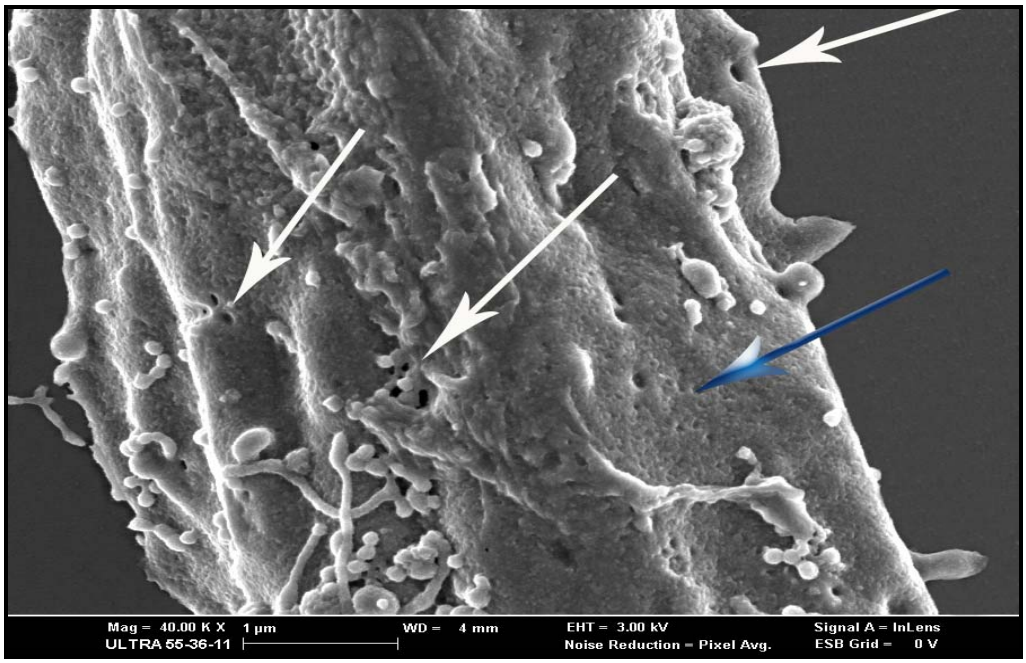

Figure 5.20: Skeletal muscle cells exposed to 0.02mg/ml CoQ10. **a**): An intact spindle-shaped cell with extending bipolar ends. **b**): The membrane surface is relatively smooth and intact (blue arrow), with rough patches. Numerous ion channels can be seen (thick white arrows).

a)

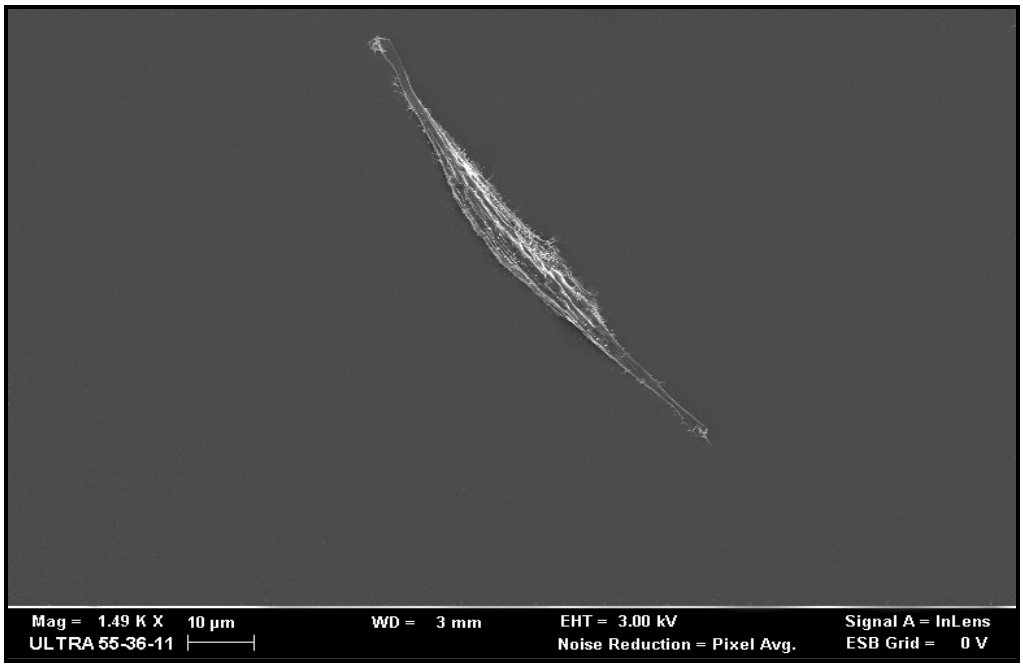

b)

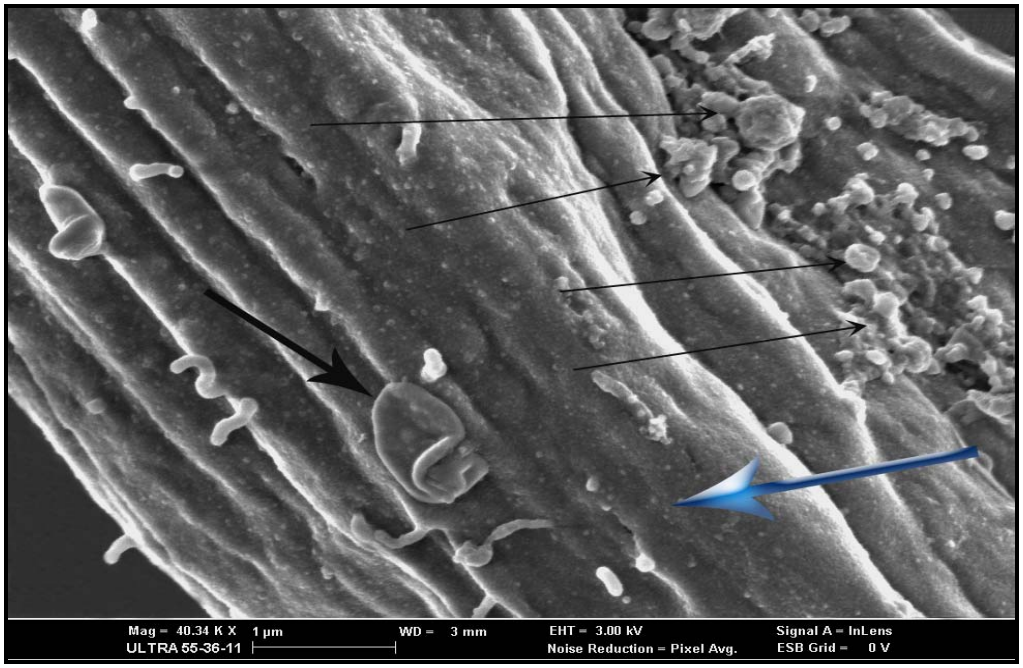

Figure 5.21: Cardiac muscle cells exposed to 0.02mg/ml CoQ10. **a**): A perfectly intact cardiac muscle cell at low magnification. **b**): The membrane is intact and smooth (blue arrow). Protein precipitations (thin black arrows) and artefacts (thick black arrow) are present.

a)

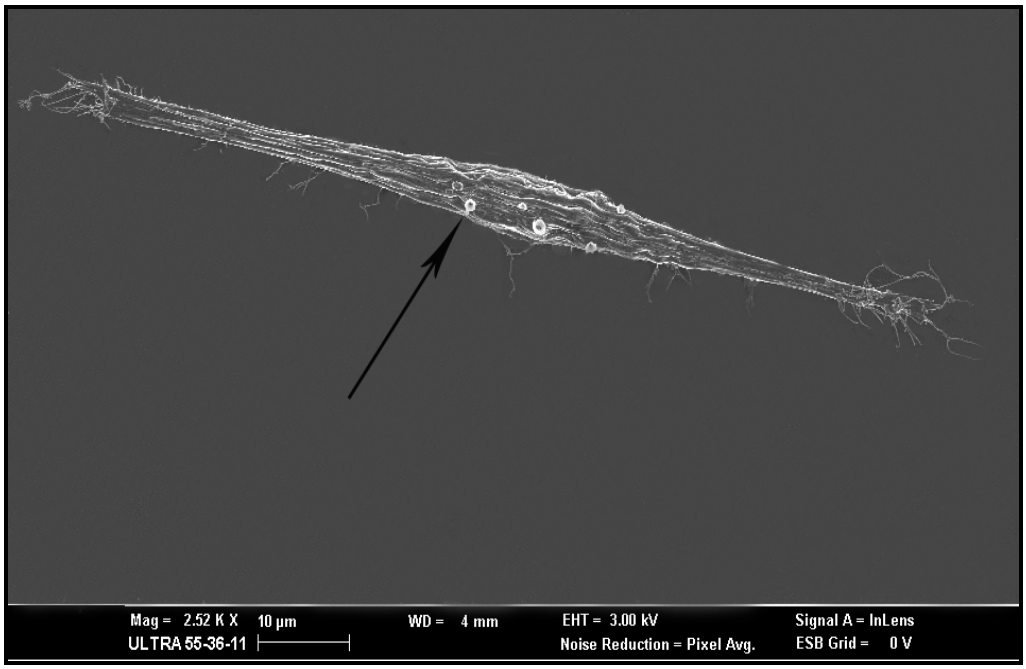

b)

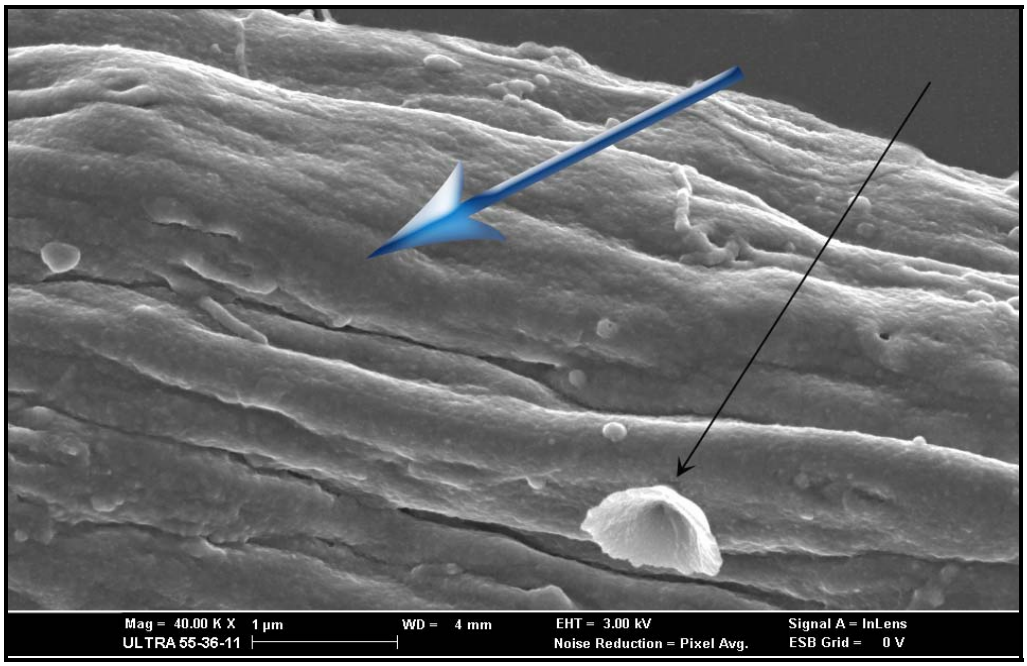

Figure 5.22: Skeletal muscle cells exposed to 0.01mg/ml CoQ10. **a**): Intact skeletal muscle cell with bipolar ends. **b**): The membrane surface appear smooth and intact (blue arrow). Ruthenium artefact is present (thin black arrow).

a)

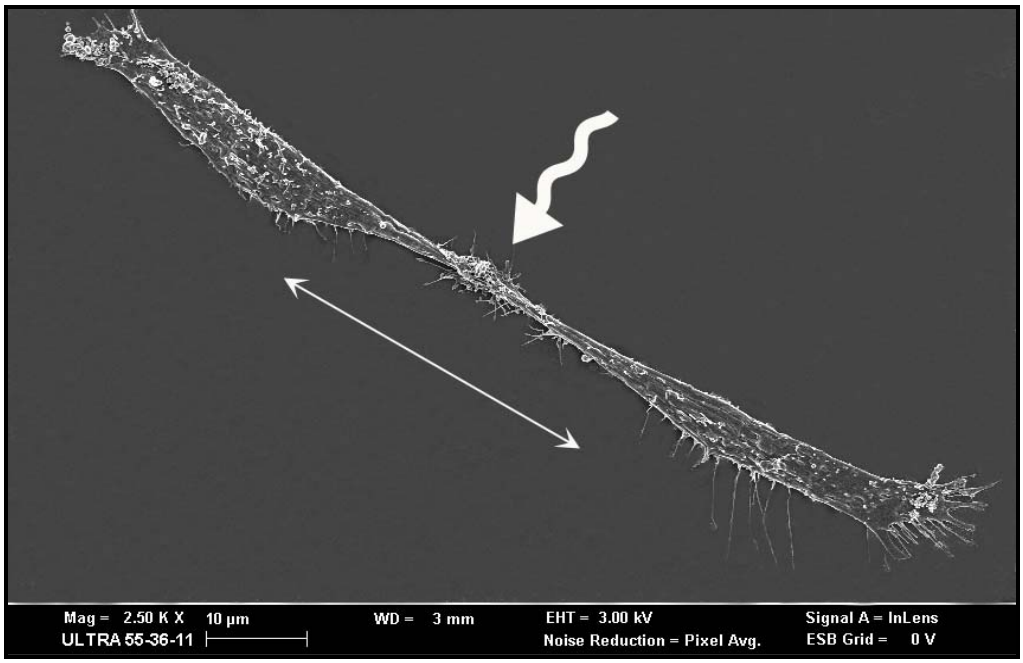

b)

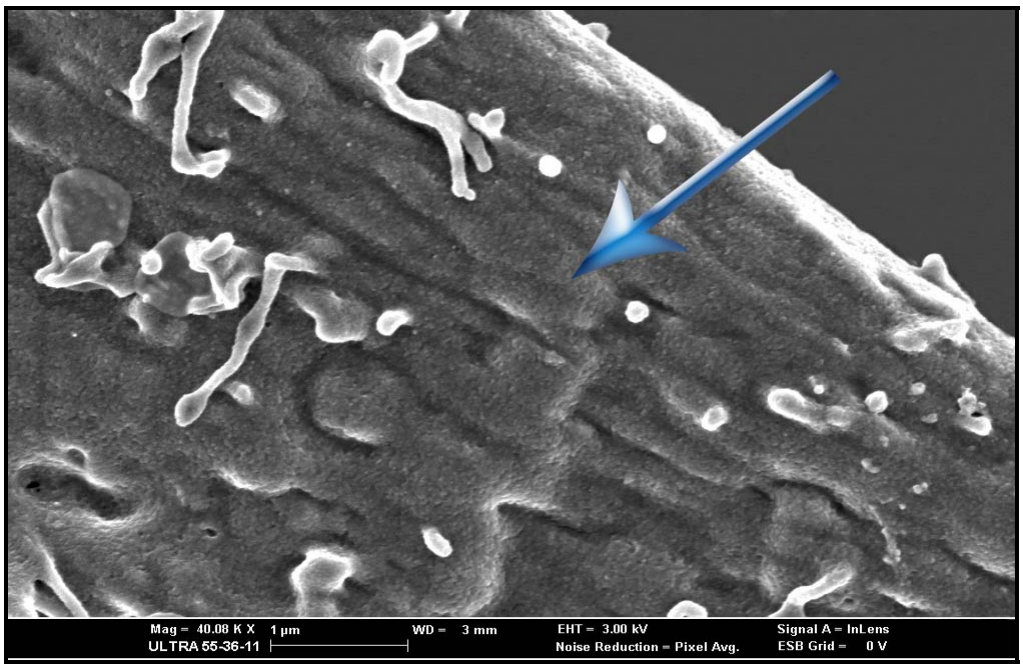

Figure 5.23: Cardiac muscle cells exposed to 0.01mg/ml CoQ10. **a**): Two fusing myoblasts. **b**): A smooth intact membrane surface (blue arrow).

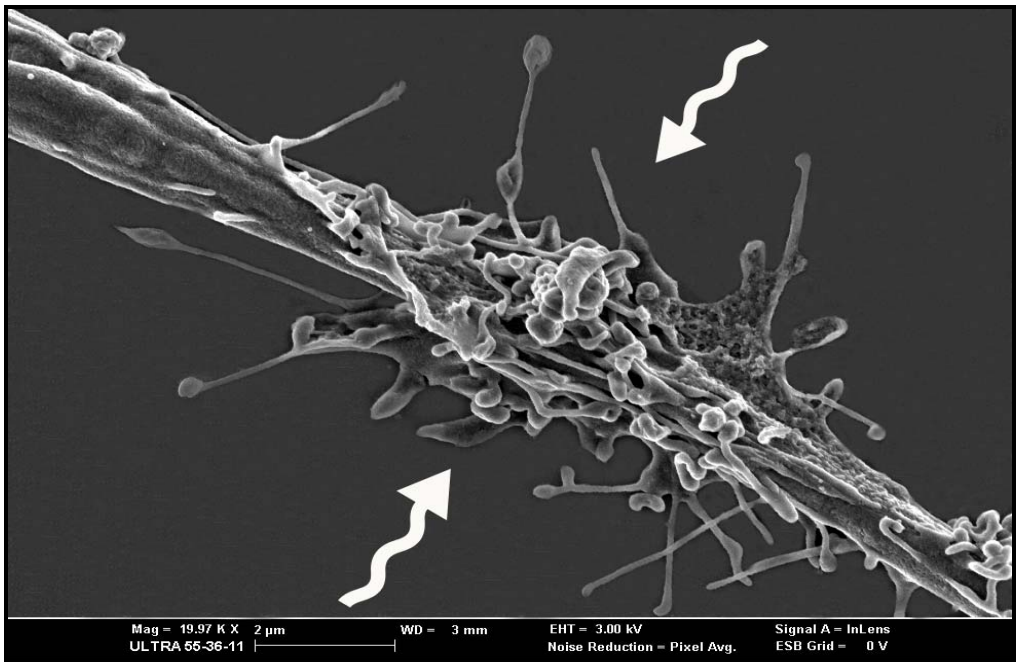

Figure 5.24: The connection between the two myoblasts in Figure 5.22 **a**. The interaction of these microprocesses with each other, or with cell bodies, establishes a connection between the cells resulting in the union of their respective filamentous systems. Presumably the microconnection between two cells develops into a cytoplasmic bridge which facilitates the integration of the filament network of both cells into a syncytium (Singer *et al*., 1984).

5.3.4 Cells Exposed to Triton X-100 after Pre-treatment with CoQ10

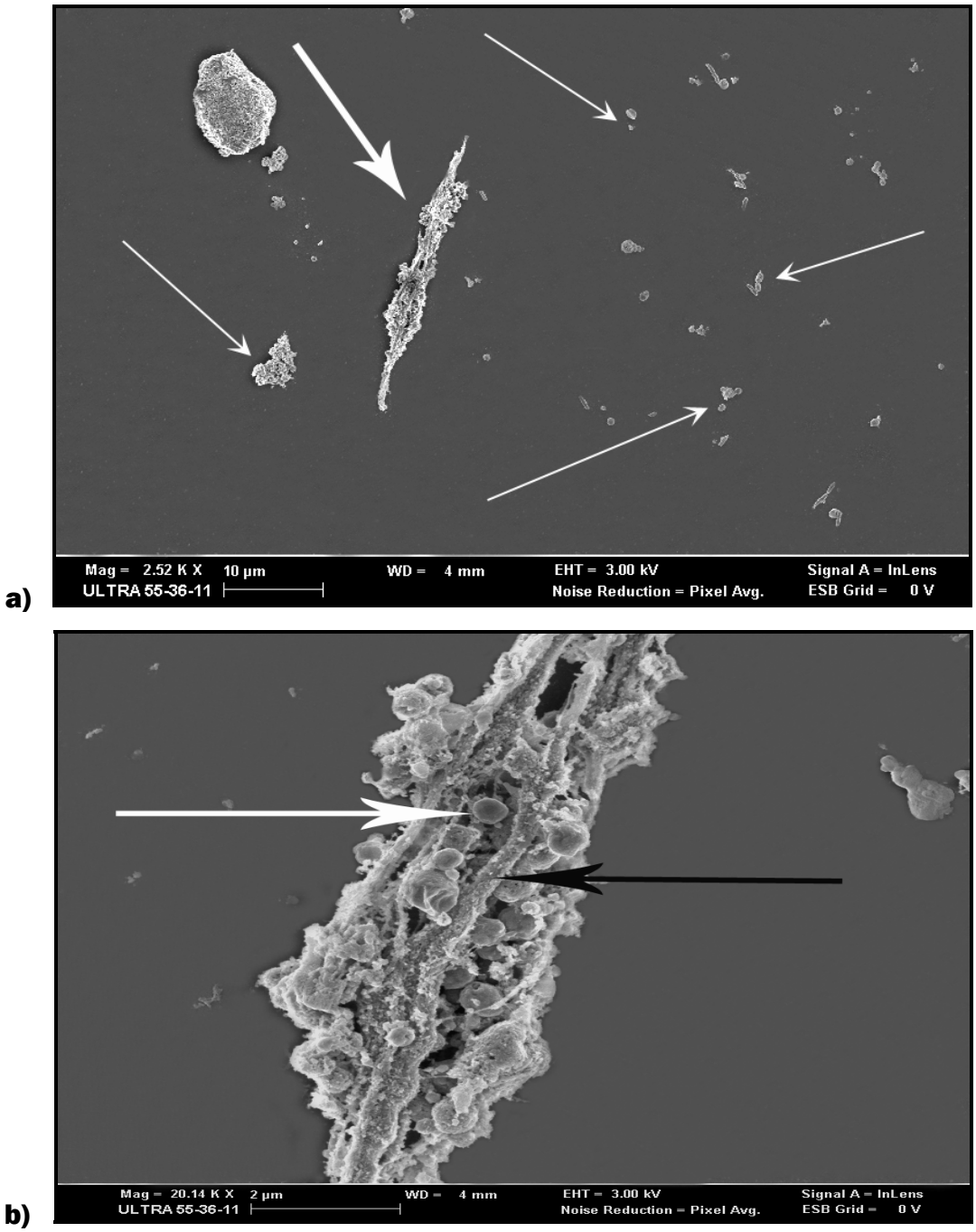

Figure 5.25: Cardiac muscle cells exposed to 0.05% Triton X-100 two hours after treatment with 0.2mg/ml CoQ10. Complete membrane lyses were seen. **a**): Part of a cell (thick white arrow) and cell debris (thin white arrows). **b**): Cytoskeleton exposed (arrows indicate the circular and cable protein structures which are insoluble to Triton X-100).

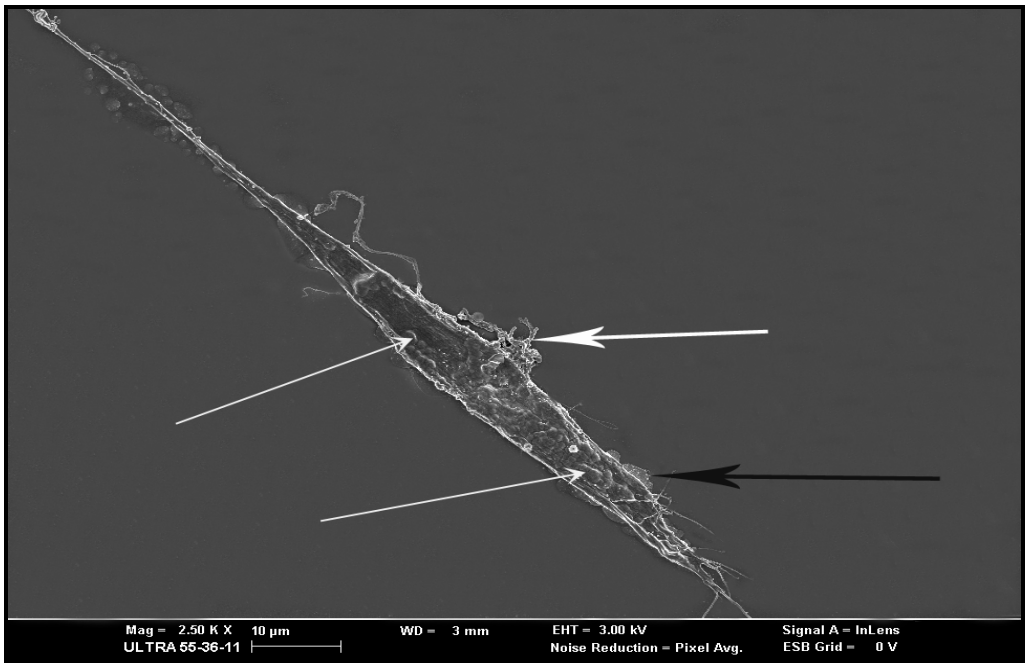

a)

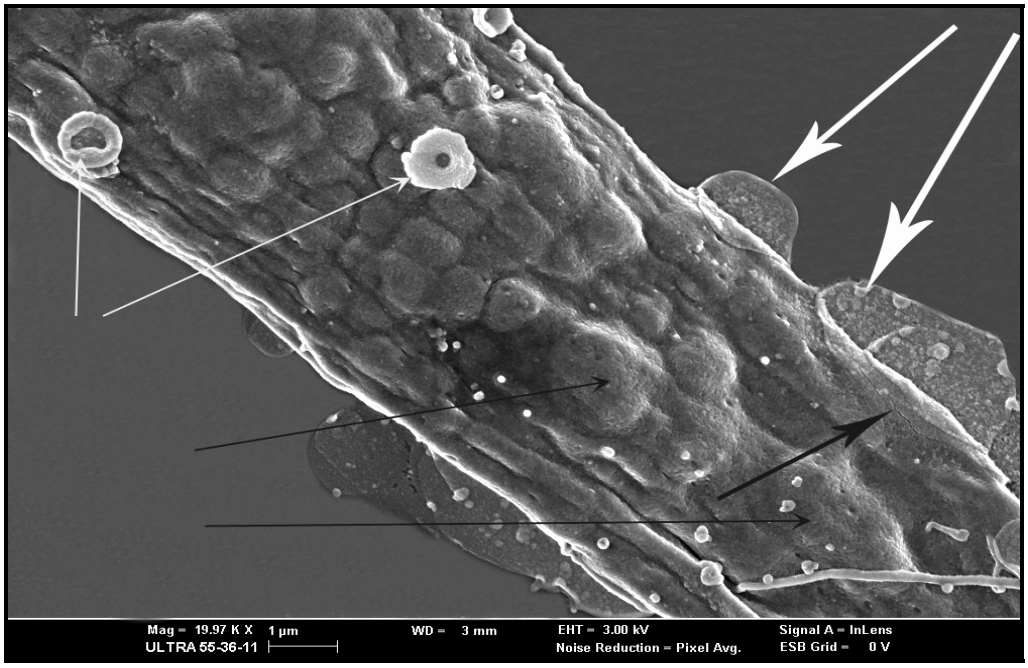

b)

Figure 5.26: Skeletal muscle cells exposed to 0.05% Triton X-100 two hours after treatment with 0.2mg/ml CoQ10. **a**): Low magnification shows membrane blebbing (thin white arrows), leakage of cytoplasmic constituents (thick white arrow & thick black arrow). **b**): Higher magnification clearly shows membrane blebs (thin black arrows) due to apoptotic changes in the cell, cytoplasmic constituents leaking through a possible rupture in the membrane (thick black & white arrows). Ruthenium artefacts (thin white arrows).

a)

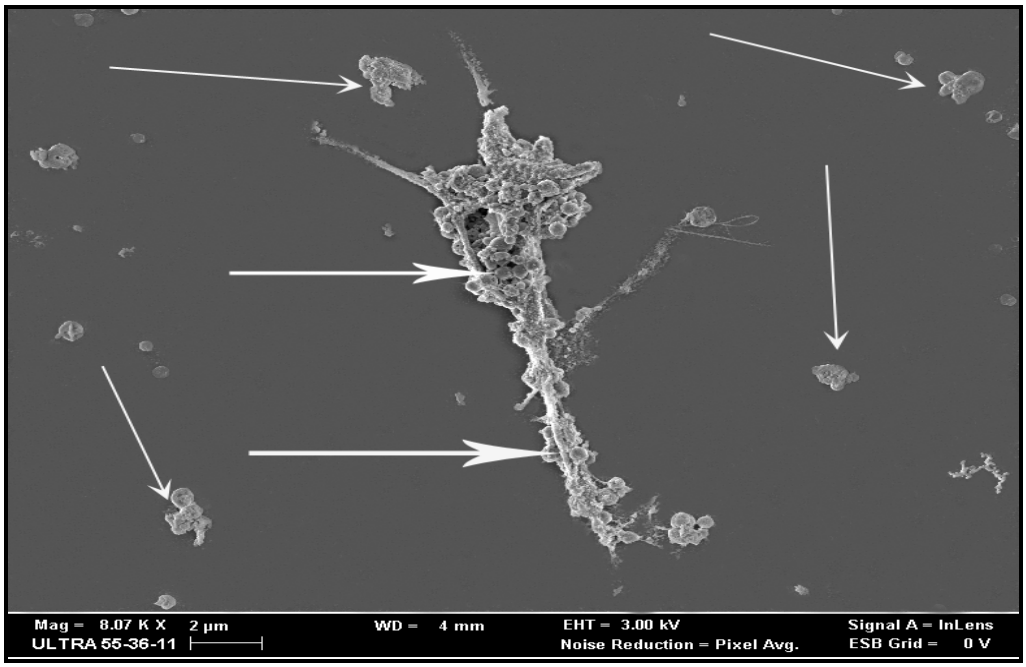

b)

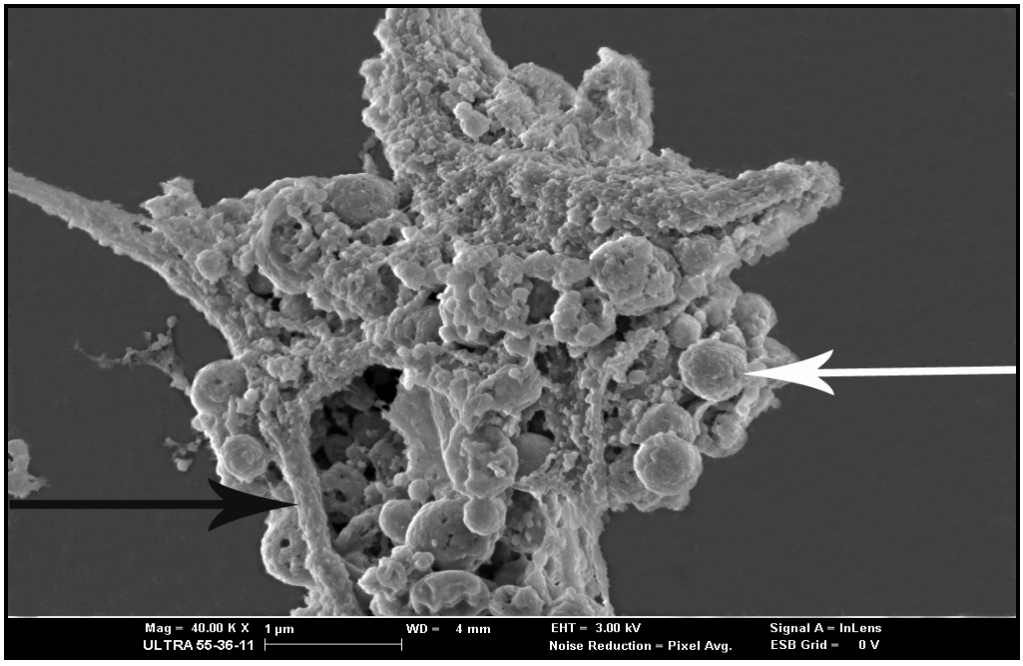

Figure 5.27: Cardiac muscle cells exposed to 0.05% Triton X-100 after pre-treatment with 0.1mg/ml CoQ10. **a**): Low magnifications shows a part of a cell (thick white arrow) and cellular debris (thin white arrows) lying around. **b**): The cell membrane is completely lysed. Insoluble proteins of the cytoskeleton (filament bundles or cables as described by Fulton *et al*., 1981 and acetylcholine receptor protein clusters as described by Connoly, 1984) are exposed (indicated by thick black and white arrows).

a)

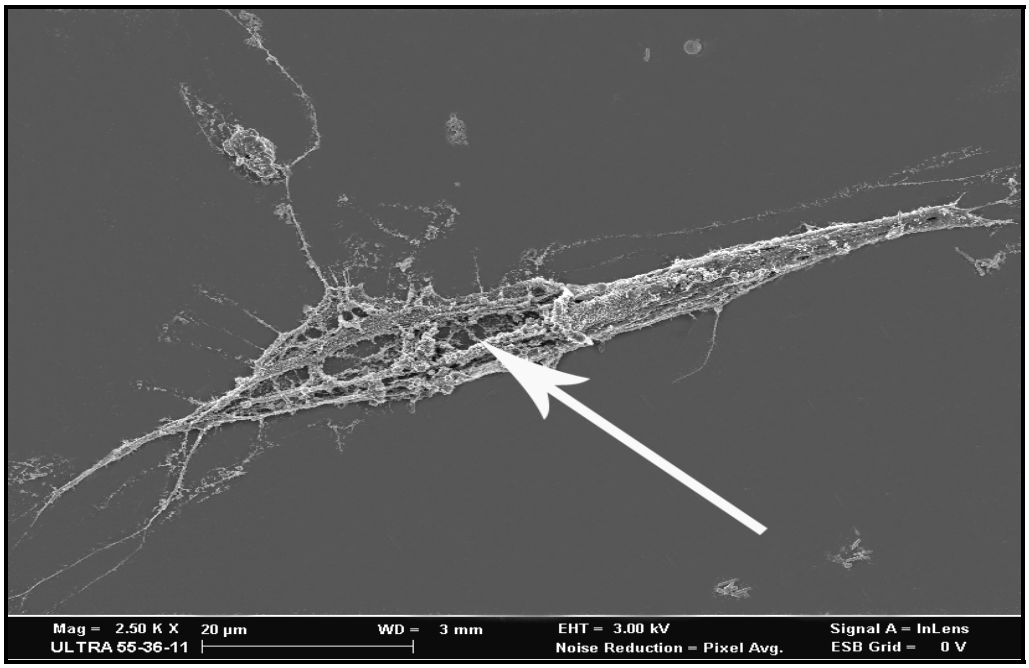

b)

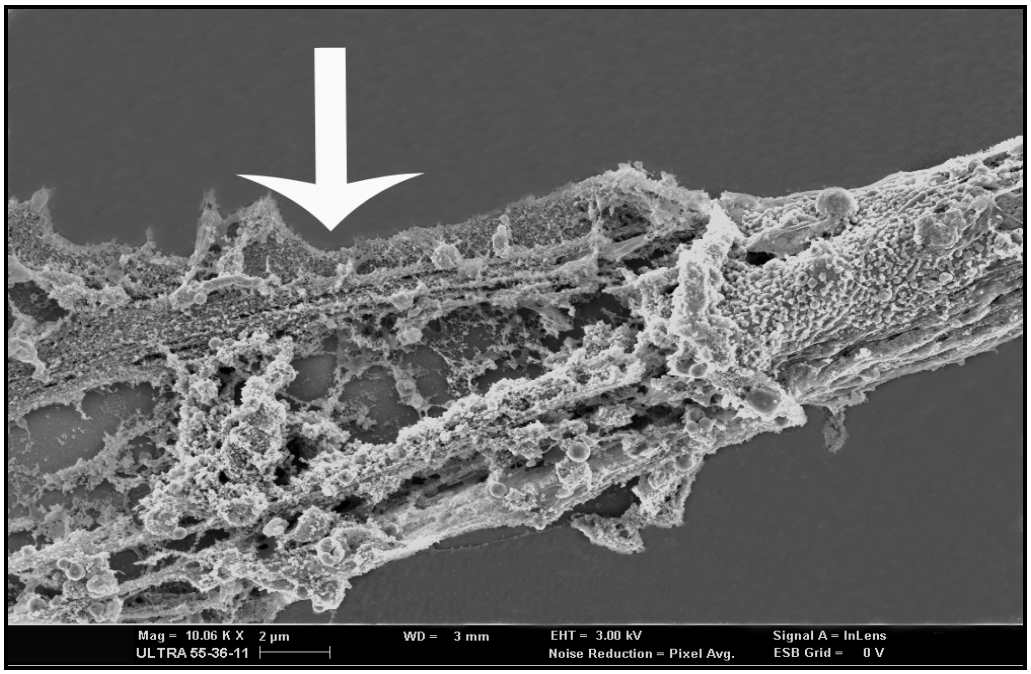

Figure 5.28: Skeletal muscle cells exposed to 0.05% Triton X-100, after being pre-treated with 0.05mg/ml CoQ10. **a**): A cell with bipolar ends and extending microprocesses. Half of the cell is still surrounded by the surface lamina, but the membrane is lysed. **b**): Major filament bundles or cables extending from deep within the cytoplasmic structure to the outer cell periphery traversing large, nearly empty regions (Fulton *et al*., 1981).

a)

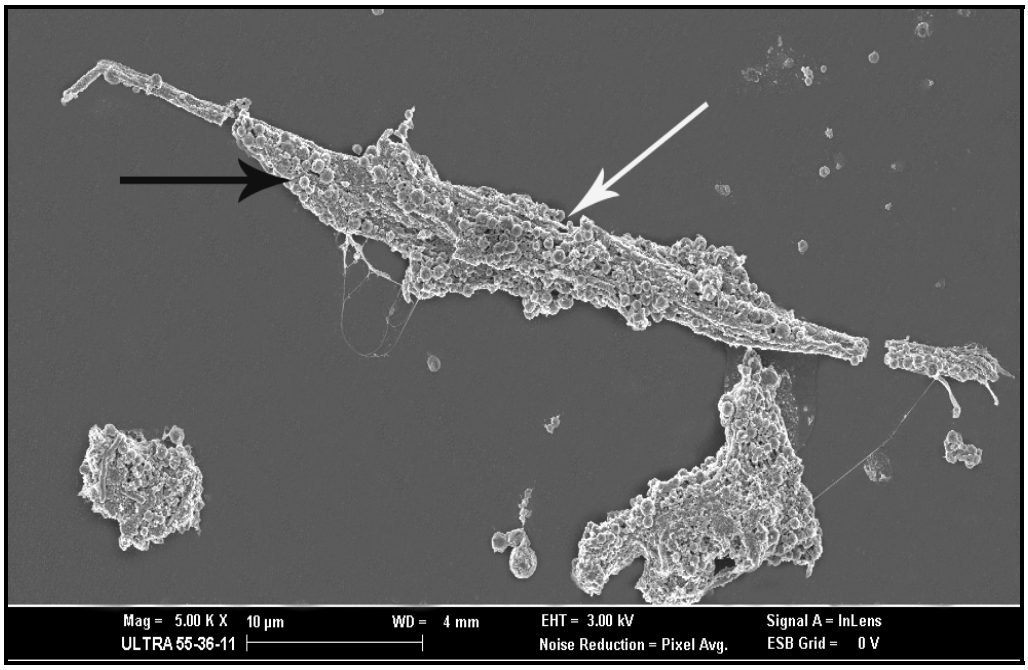

b)

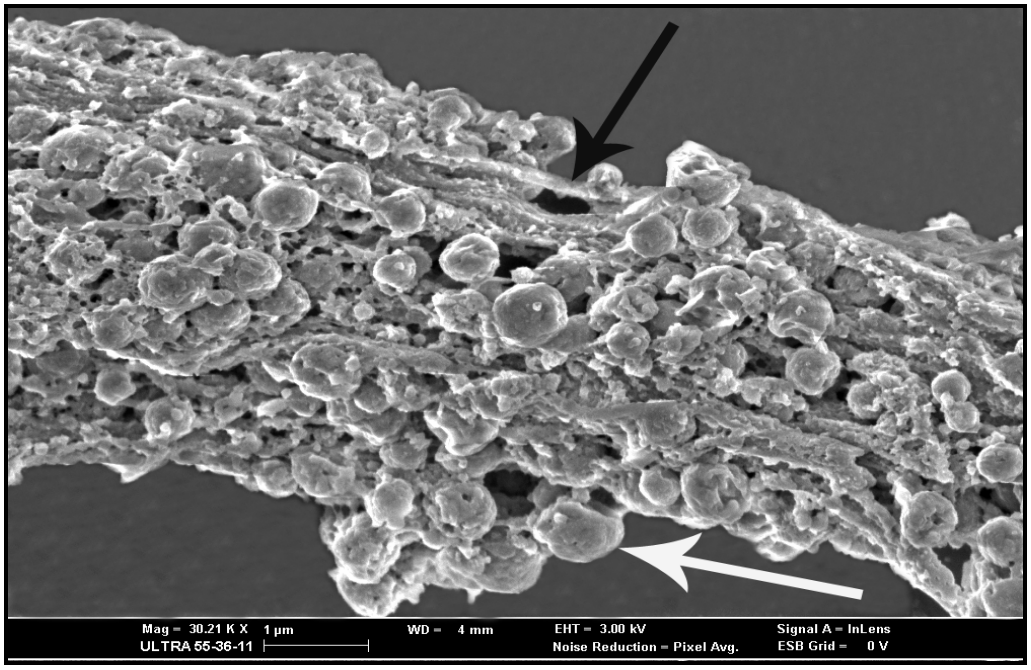

Figure 5.29: Cardiac muscle cells exposed to 0.05% Triton X-100, after being pre-treated with 0.05mg/ml CoQ10. **a**): Complete membrane lyses were seen with cell debris lying around. **b**): The filament bundles or cables (thick black arrow) described by Fulton *et al*., 1981. The circular structure indicated by the white arrow is protein constituents of the cytoskeleton, possibly acetylcholine receptor clusters described by Connoly, 1984, insoluble to Triton X-100.

Notable structures in the postproliferative myoblast are the major filament bundles or cables extending from deep within the cytoplasmic structure to the outer cell periphery (Fulton *et al*., 1981). These cables (Figure 5.27 & 5.29 **b**, black arrow), traversing large, nearly empty regions (Figure 5.28 **b**), are characteristic of and always found in postproliferative myoblasts (Fulton *et al*., 1981). In myoblasts preparing to fuse, both the surface lamina and the internal networks show highly specific spatial rearrangement; in addition, the internal networks become more extractible. After fusion, both the internal networks and the surface lamina rapidly reorganize in a stable arrangement as the muscle cell begins to construct the extensive contractile apparatus, thus a critical stage in muscle development is accompanied by rapid, extensive, and transient reorganization of skeletal framework and its surface lamina (Fulton *et al*., 1981).

Before innervations of the muscle cell (both *in vivo* and *in vitro*) acetylcholine receptors are widely distributed over the surface of the myotube, but once the nerve cell contacts the myotube, there is a reorganization of the acytylcholine receptors and the clusters under the nerve process innervating that muscle cell (Connoly, 1984). Tank *et al*., 1982, found that when blebs are induced in L6 myotubes, the acetylcholine receptors in these blebbed regions are free to diffuse in the plane of the membrane, whereas receptors in intact cell membranes are much more constrained, with some fractions virtually nondiffusible. They proposed that bleb formation mechanically broke connections anchoring these receptors to the cytoskeleton (Tank *et al*., 1982). Prives *et al*., 1980 and 1982, found that the majority of acetylcholine receptors were retained on the insoluble cytoskeleton after detergent extraction of cells. Stya *et al*., 1983, found a correlation between the average mobility of acetylcholine receptors in the plane of the membrane and their extractability by Triton X-100. Both of these studies concluded that clustered receptors were attached to the cytoskeleton. The results of the study by Connoly, 1984, supported the hypothesis of the attachment of acetylcholine receptors to a submembranous cytoskeleton. They further proposed that receptor clusters are stabilized by actin-containing filaments within the cytoplasm, because existing clusters could not be destabilized with Colcemid, therefore, cluster stability is not dependent on microtubules, but the movement of receptors in the plane of the membrane (Connoly, 1984).

a)

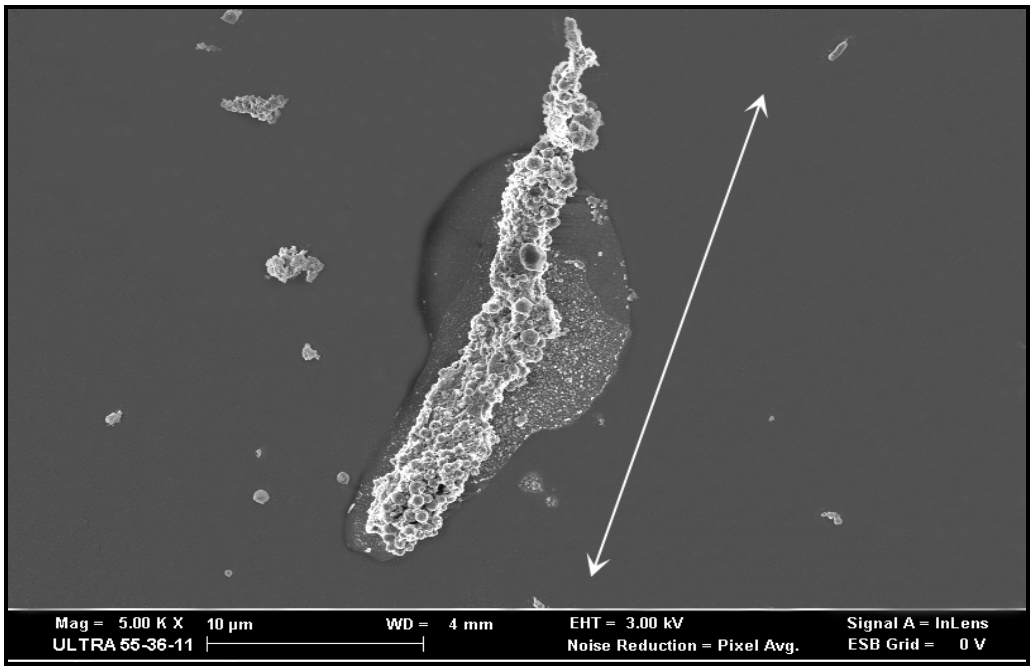

b)

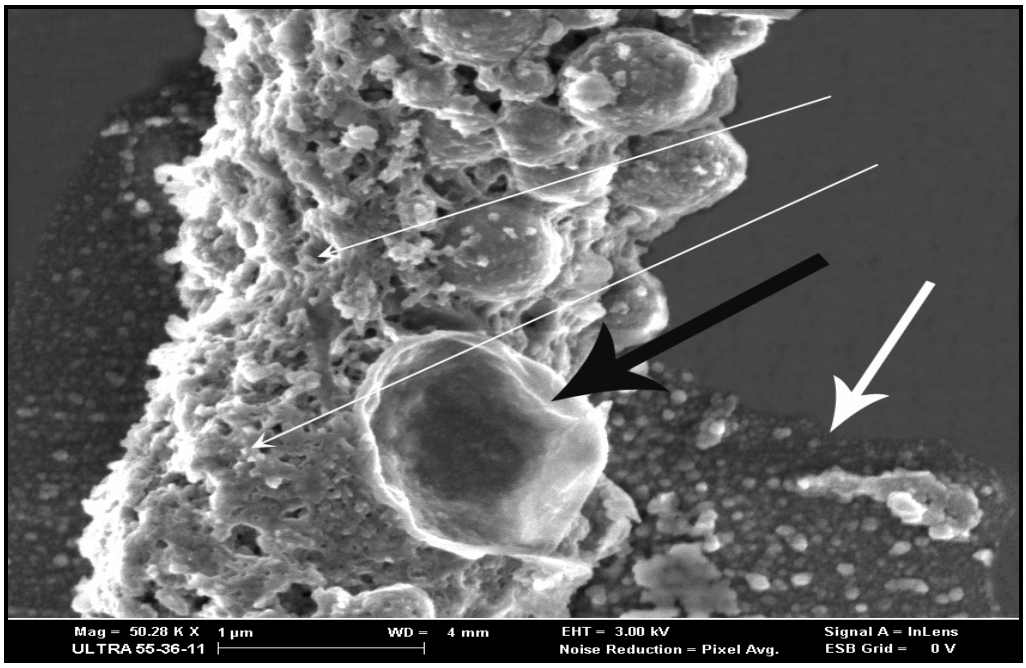

Figure 5.30: Cardiac muscle cells exposed to 0.05% Triton X-100 after 0.02mg/ml CoQ10 pre-treatment. **a**): Part of a cell with lysed membrane can be seen. Cell debris lying in the vicinity. **b**): Components (possibly a remnant of an apoptotic body or a protein cluster) of the cytoskeleton are visible (thick black arrow). Leakage of cytoplasm indicated by thick white arrow. The plasma lamina is disrupted but still present (thin white arrows).

a)

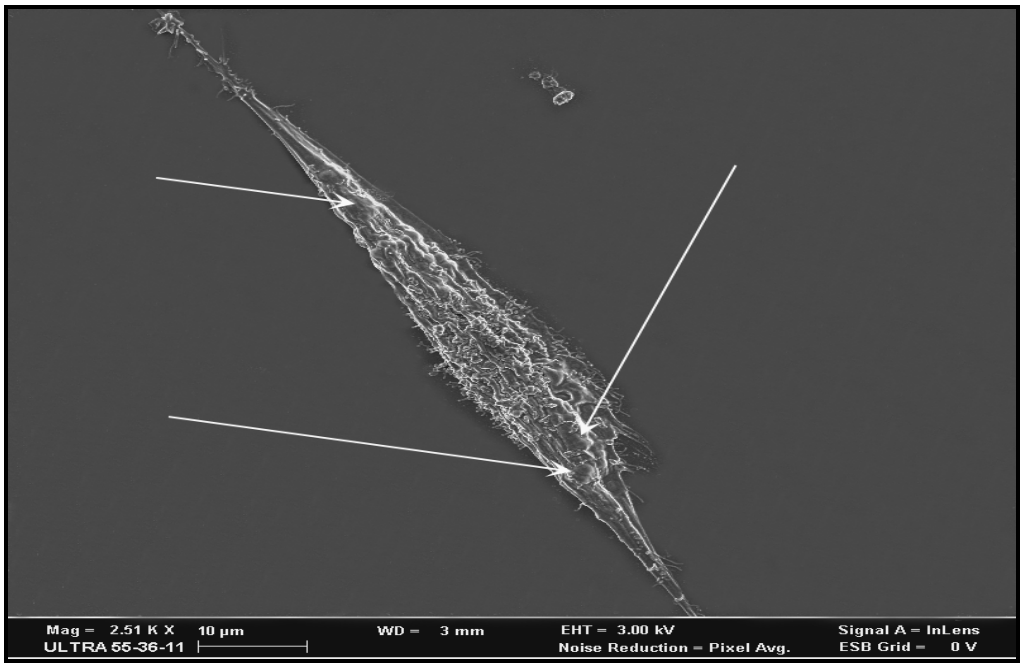

b)

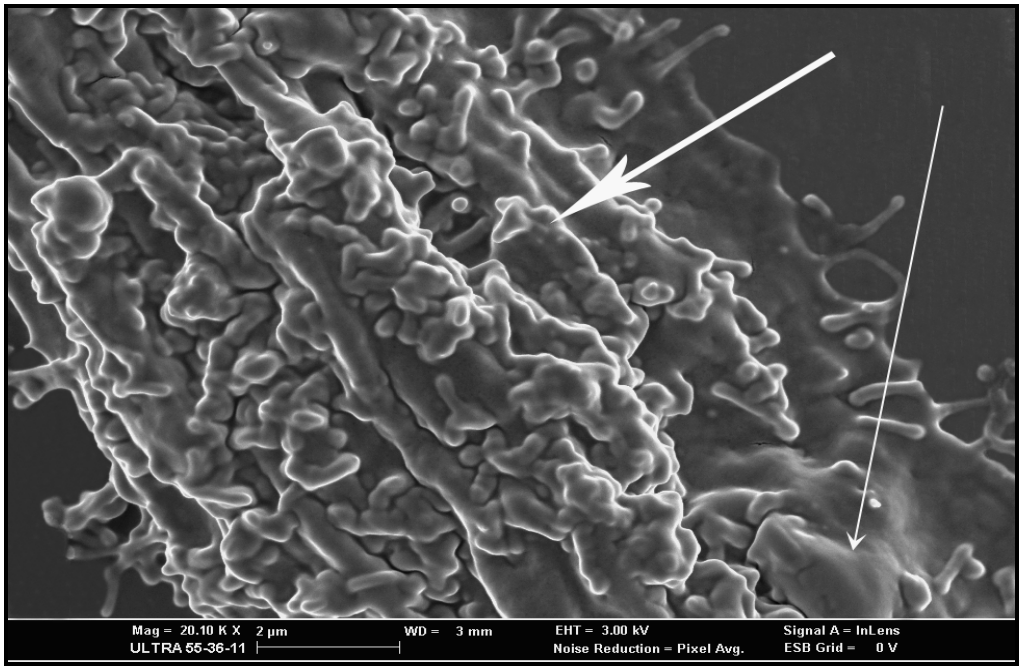

Figure 5.31: Skeletal muscle cells exposed to 0.005% Triton X-100 after pre-treatment with 0.2mg/ml CoQ10. **a**): Membrane blebs were seen at low magnification (thin white arrows). **b**): Higher magnification shows a shrunken membrane (thick white arrow) and membrane blebbing (thin white arrow), characteristic of a cell in which the process of apoptosis is present.

a)

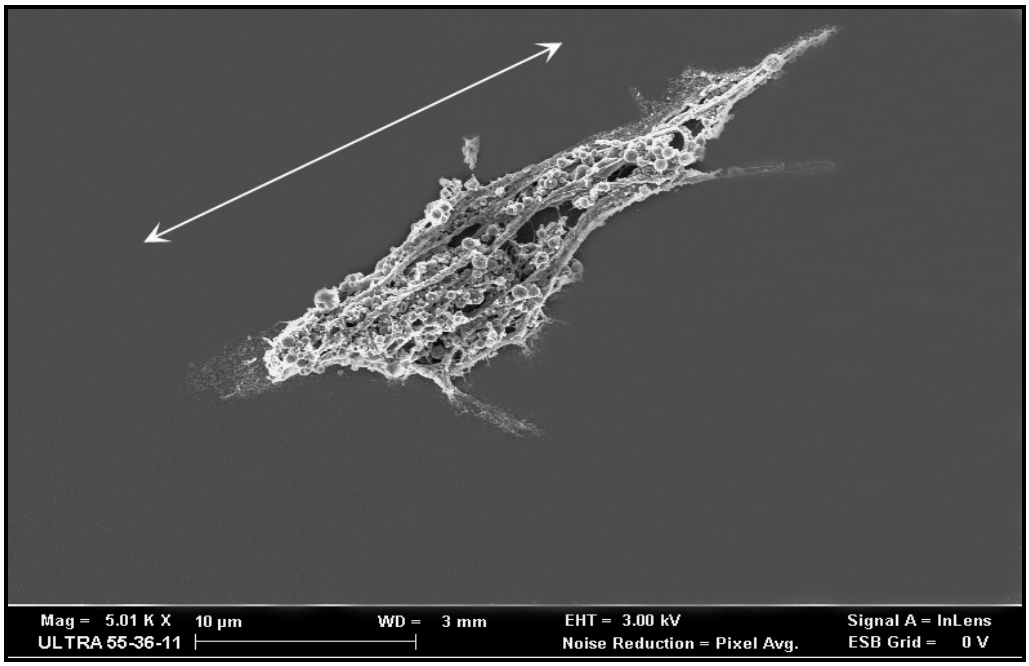

b)

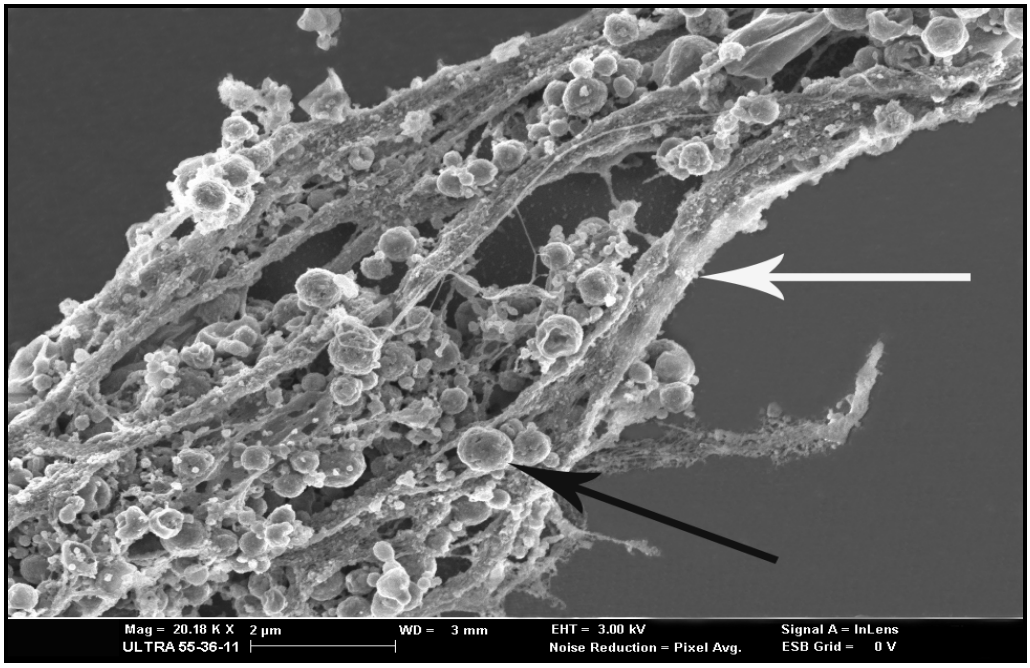

Figure 5.32: Cardiac muscle cells exposed to 0.005% Triton X-100 after pre-treatment with 0.2mg/ml CoQ10. **a**): Complete membrane lyses were seen at low magnification. **b**): Filament bundles and clusters (thick black and white arrows) traversing empty spaces can be seen at high magnification.

a)

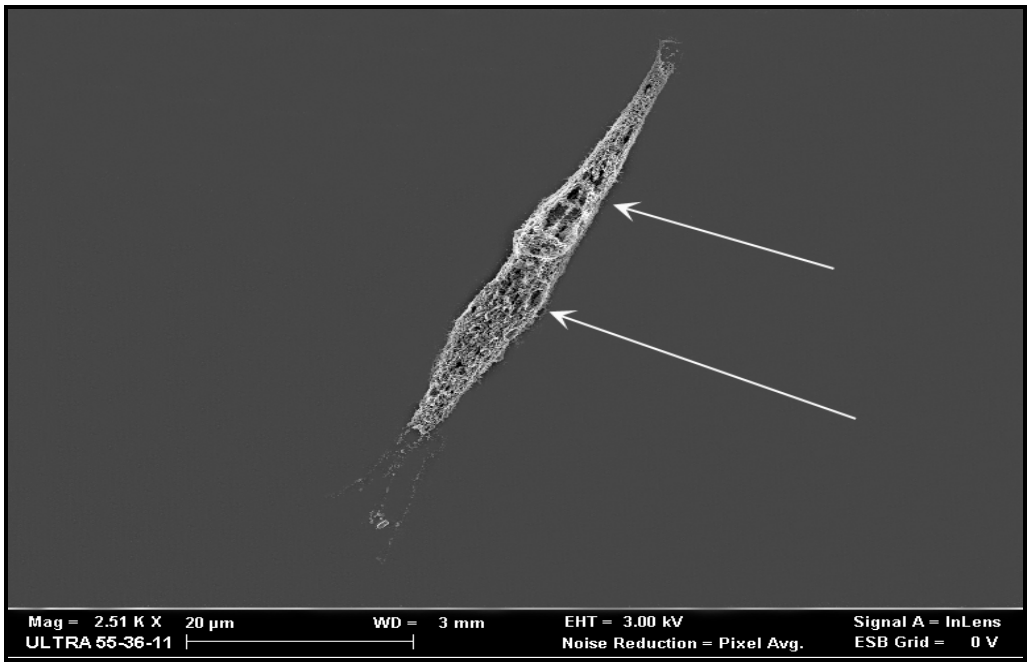

b)

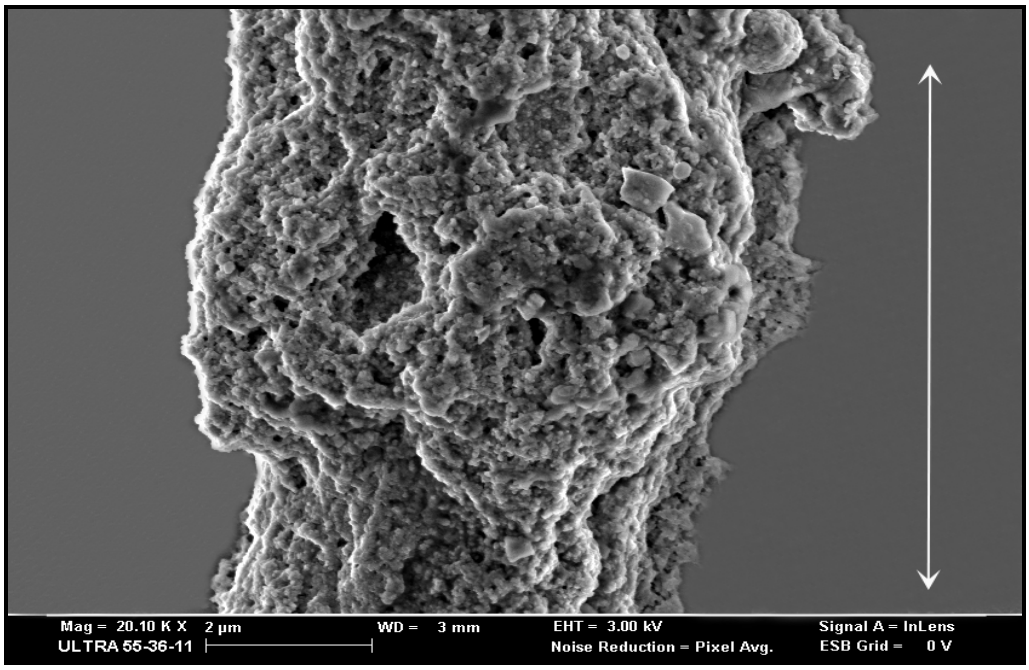

Figure 5.33: Skeletal muscle cells exposed to 0.005% Triton X-100 after pre-treatment with 0.1mg/ml CoQ10. Membrane lyses were seen. Plasma lamina were present but largely disrupted. **a**): Empty spaces (thin white arrows).

a)

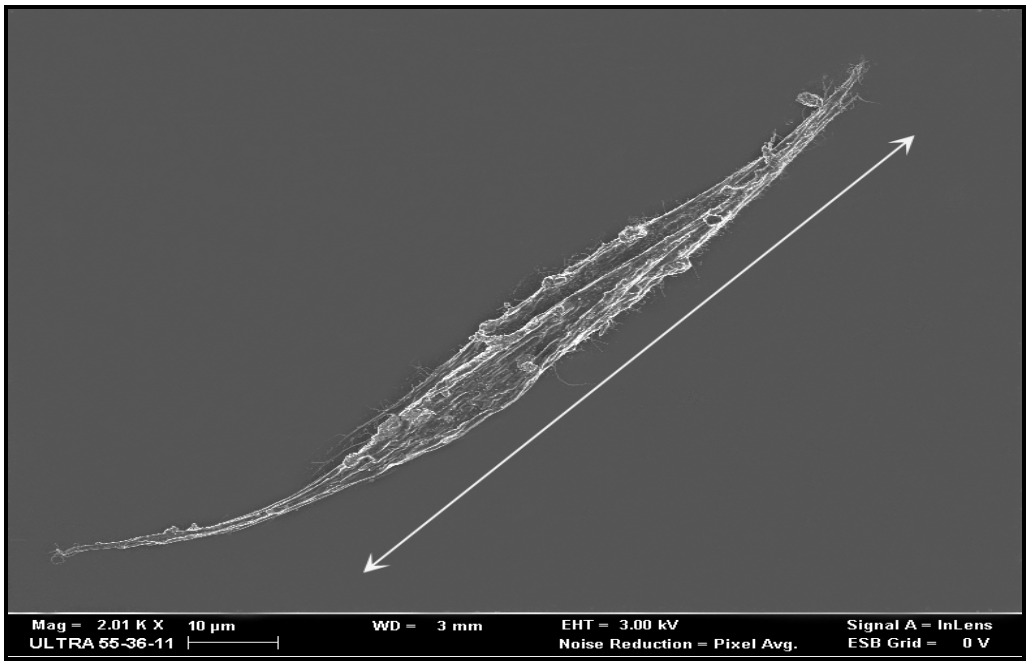

b)

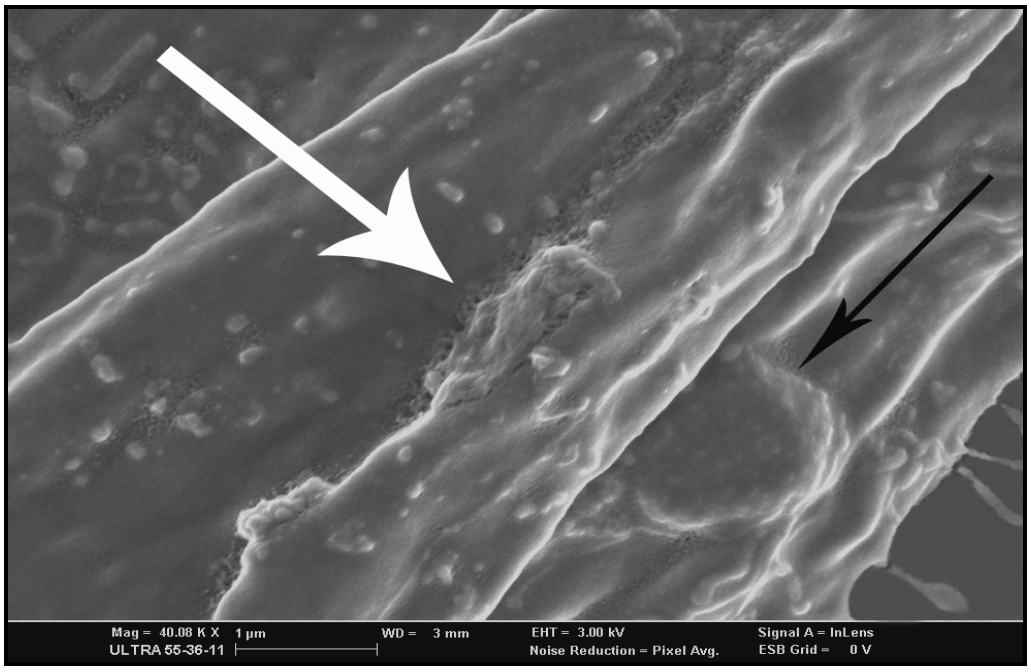

Figure 5.34: Cardiac muscle cells exposed to 0.005% Triton X-100 after pre-treatment with 0.1mg/ml CoQ10. **a**): Bipolar ends extending from the spindle-shaped cell. Cell seems largely intact. **b**): High magnification shows an intact membrane with bulging (black arrow), and a rare appearance of a "***membrane patch"*** on a part of the membrane that present more rough and slightly damaged (thick white arrow).

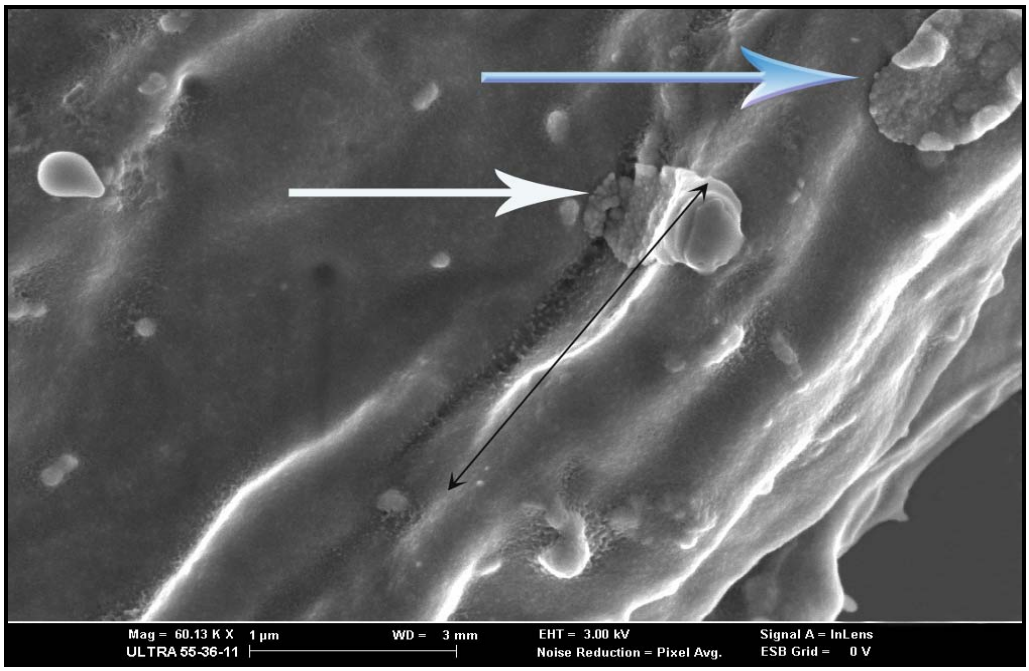

Figure 5.35: Higher magnification of Figure 5.34 **a**. The thin black arrow shows a part in the membrane that looks like a tear, on part of the tear is a patch (thick white arrow). The blue arrow indicates a patch-like formation on the surface of the cell membrane which appears to have the same structural composition as the membrane itself.

Disruption of the plasma membrane is a common event in various normal animal cells, and membrane-repair machinery is essential to prevent disruption-induced cell death. In skeletal muscle, membrane disruptions are most often observed under physiological conditions, because muscle fibres contract repeatedly and are often susceptible to varying degrees of mechanical stress. The fragility of the sarcolemma makes it unable to withstand the mechanical stress, and a defective membrane-repair easily results in necrosis of the muscle fibres (Hayashi, 2003). Membrane rupture leads to exposure of hydrophobic phospholipids to the aqueous environment, an energetically unfavourable state (Lammerding *et al*., 2007). The entropic forces that draw the membrane ends together are insufficient to reseal membrane lesions larger than 1µm in nucleated cells under physiological conditions (McNeil *et al*., 2003). Membrane tension, driven by interaction of phospholipids with the underlying cytoskeleton, slows or completely blocks self sealing (Lammerding *et al*., 2007). Instead, cells utilize an active membrane-repair process based on active trafficking of endomembrane vesicles to the damage site and subsequent fusion with the plasma membrane by exocytosis. Many of the molecular details of this process remain unclear. It appears that membrane repair involves both a

reduction in membrane tension - possibly by local depolymerization of the cortical cytoskeleton - and patch formation. In the latter process, homotypic fusion of membrane vesicles creates a patch at the rupture site that then fuses with the plasma membrane in a Ca^{2+}-dependent process (Lammerding *et al*., 2007). Depending on the cell type, the vesicular membrane compartments participating in the repair may include cortical granules, yolk granules, endocytic components, lysosomes, and enlargosomes (McNeil *et al*., 2003 and 2005). The active membrane fusion process requires several membrane proteins, including SNARE proteins, a family of transmembrane proteins essential in most intracellular membrane fusion processes, and synaptotagmins, transmembrane proteins containing two highly conserved Ca^{2+}-binding domains that are thought to serve as Ca^{2+} sensors (Giraudo *et al*., 2006). Most recently, ferlins have been identified as a conserved protein family that participate in membrane repair. The ferlin family consists of four different genes that encode dysferlin, myoferlin, otoferlin, and Fer1L4; dysferlin-null cells show accumulation of membrane vesicles near the damaged membrane (McNeil *et al*., 2003 and 2005).

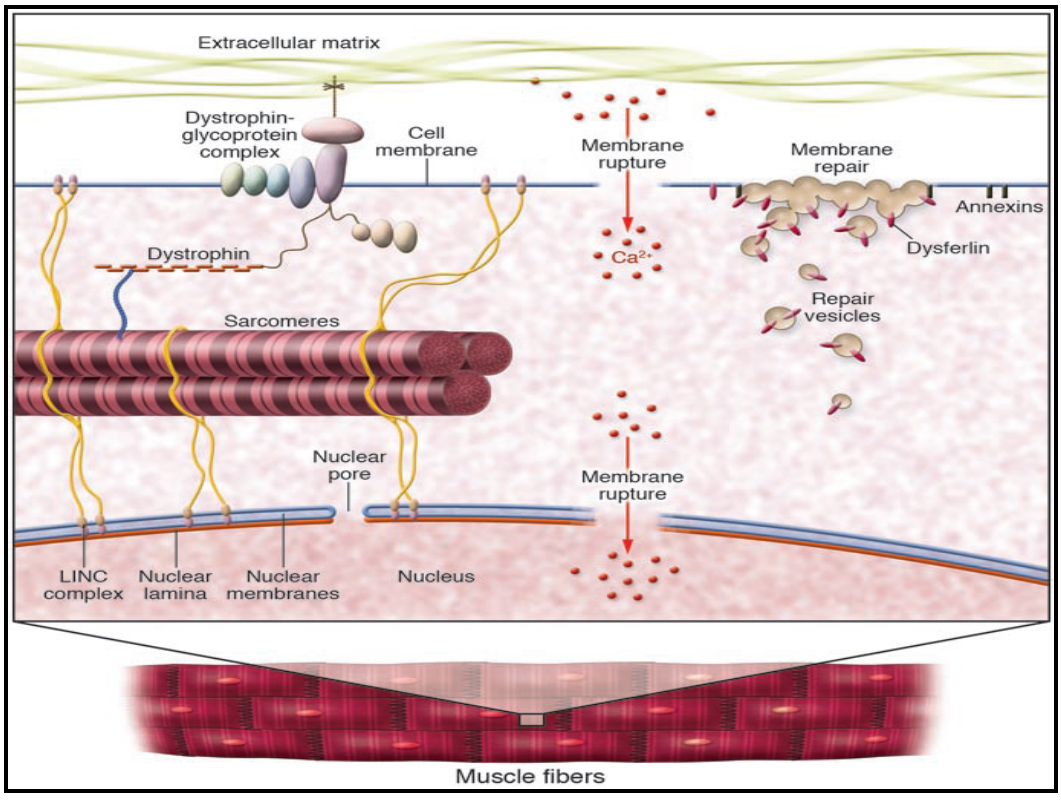

Figure 5.36: Schematic representation of the membrane repair machinery in a muscle cell as presented by Lammerding *et al*., 2007.

a)

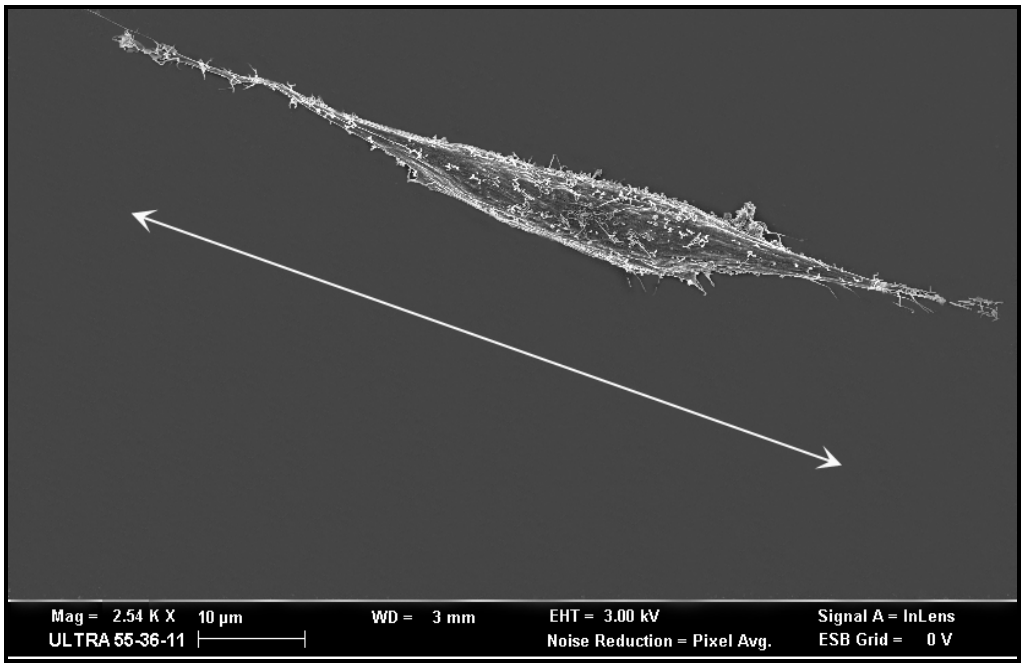

b)

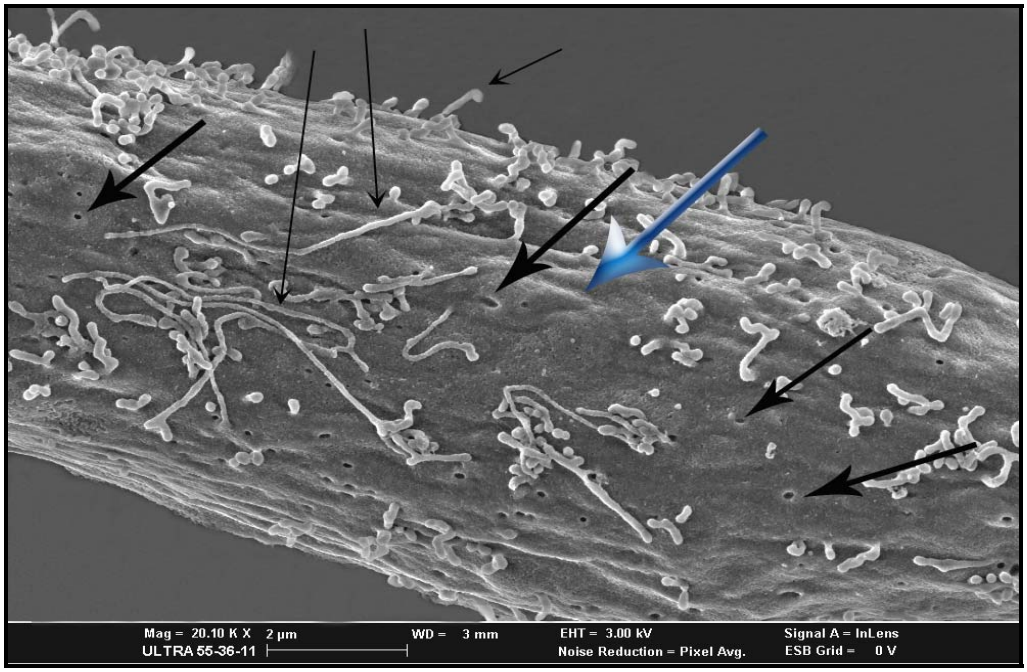

Figure 5.37: Skeletal muscle cells exposed to 0.005% Triton X-100, after pre-treatment with 0.05mg/ml CoQ10. **a**): A perfectly intact bipolar cell. **b**): Higher magnification shows and intact membrane (blue arrow) with numerous microvilli an spherical protrusions (thin black arrows), and numerous ion channels on the surface of the cell.

a)

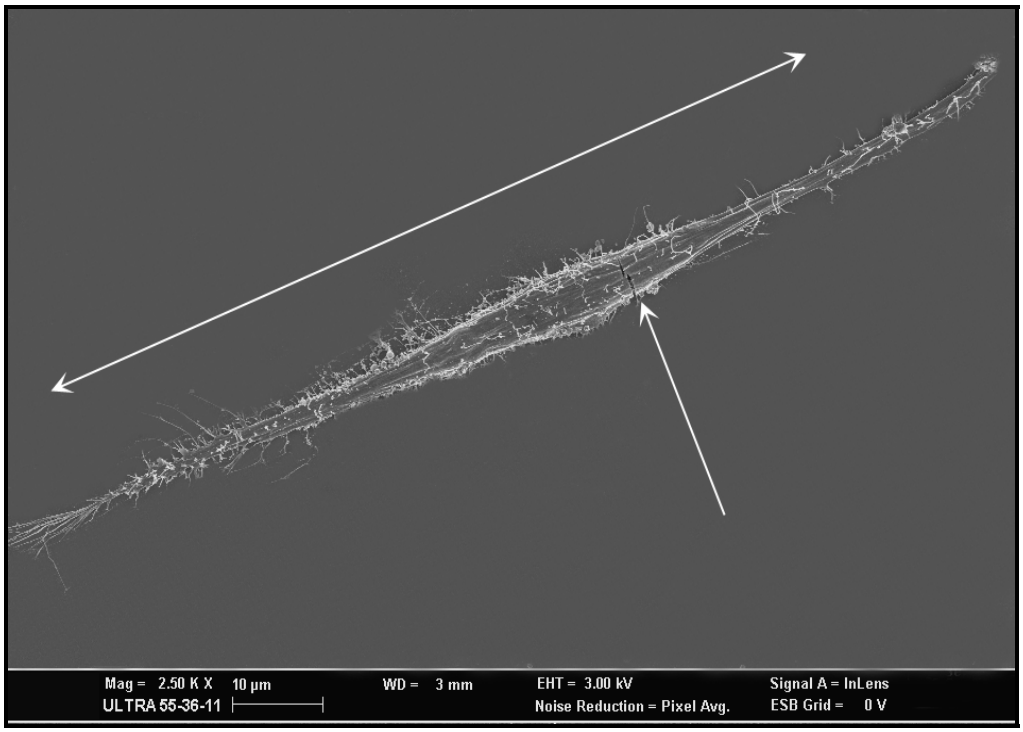

b)

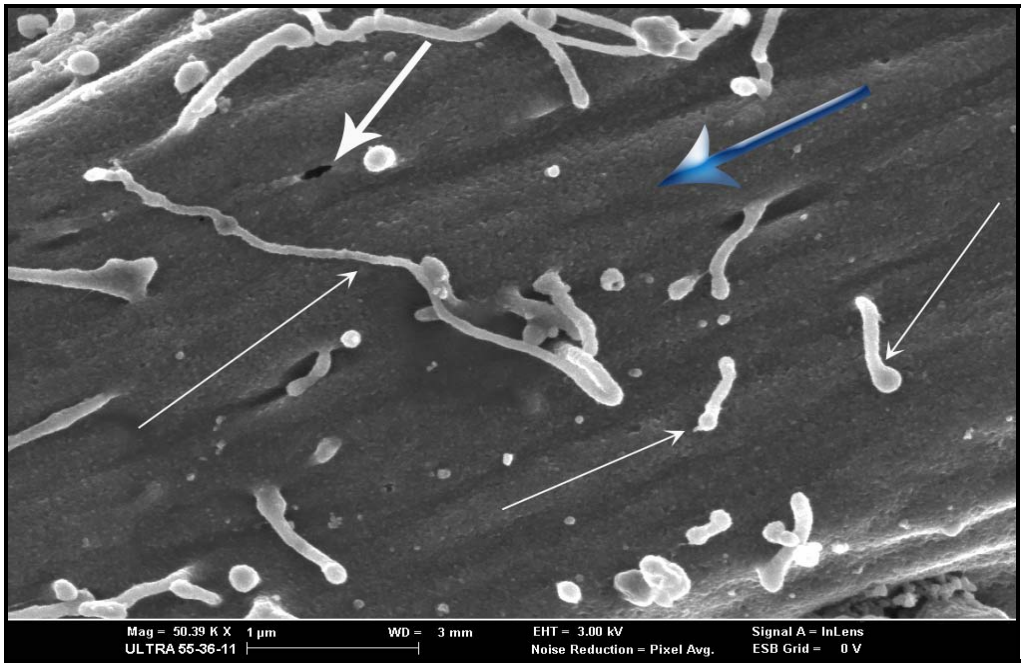

Figure 5.38: Cardiac muscle cells exposed to 0.005% Triton X-100, after pre-treatment with 0.05mg/ml CoQ10. **a**): An intact bipolar cell (double-headed arrow). Breakage of the upper tip was probably caused by critical point drying (thin white arrow). **b**): A perfectly intact membrane surface (blue arrow) with microvilli and small spherical protrusions (thin white arrows), and ion channels (thick white arrow).

a)

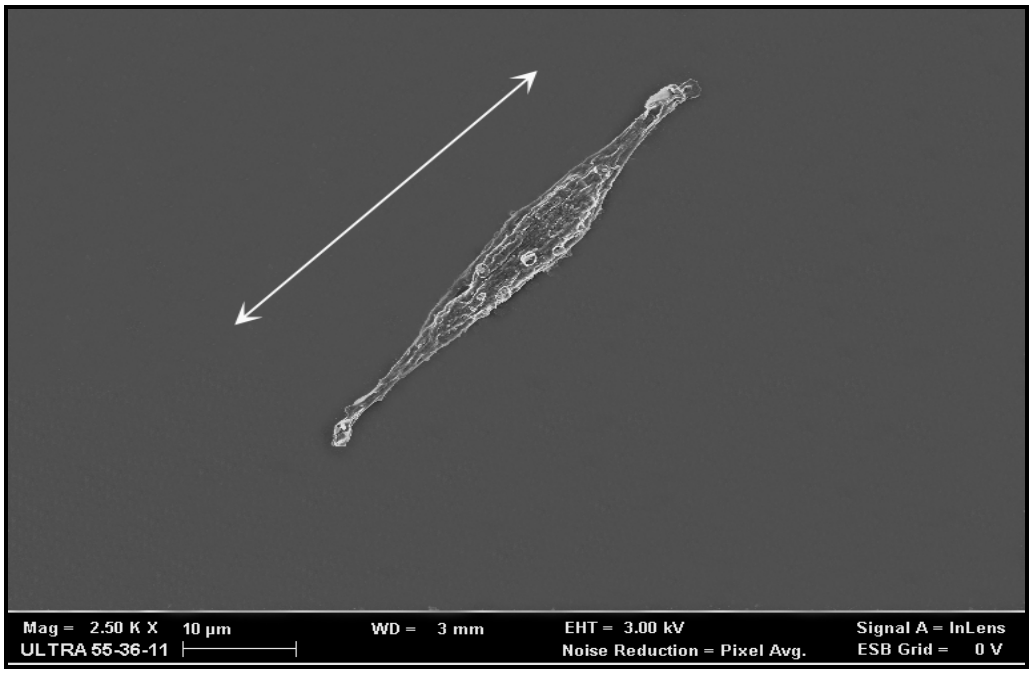

b)

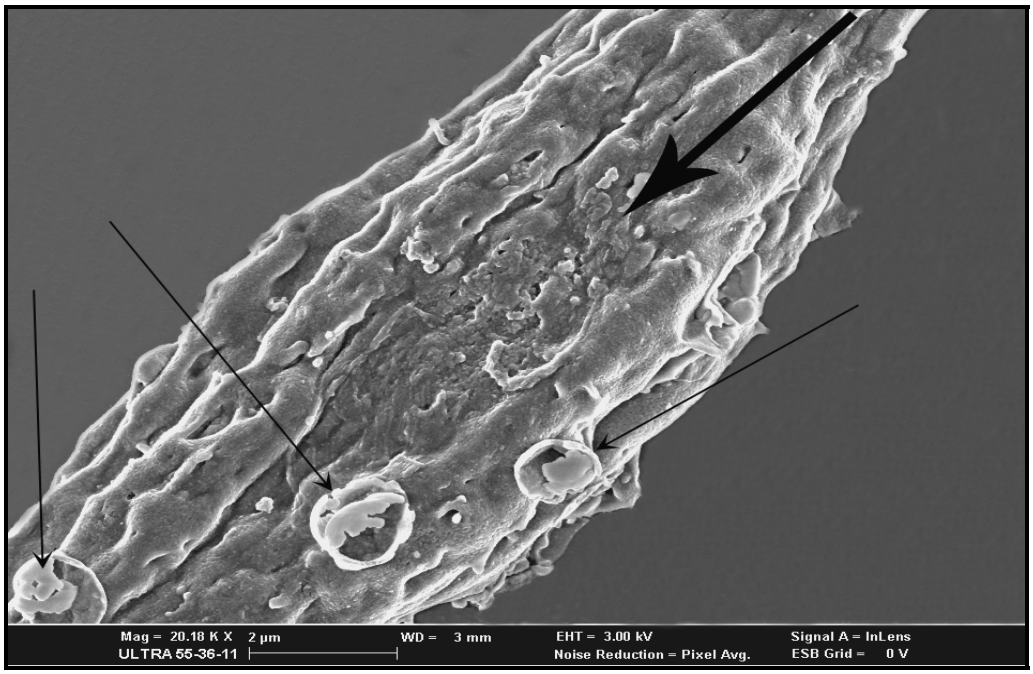

Figure 5.39: Skeletal muscle cells exposed to 0.005% Triton X-100 after pre-treatment with 0.02mg/ml CoQ10. **a**): An intact skeletal muscle cell. **b**): Cell membrane has a rough patch (thick black arrow), but seems largely intact. Presence of ruthenium artefacts were noted (thin black arrows).

a)

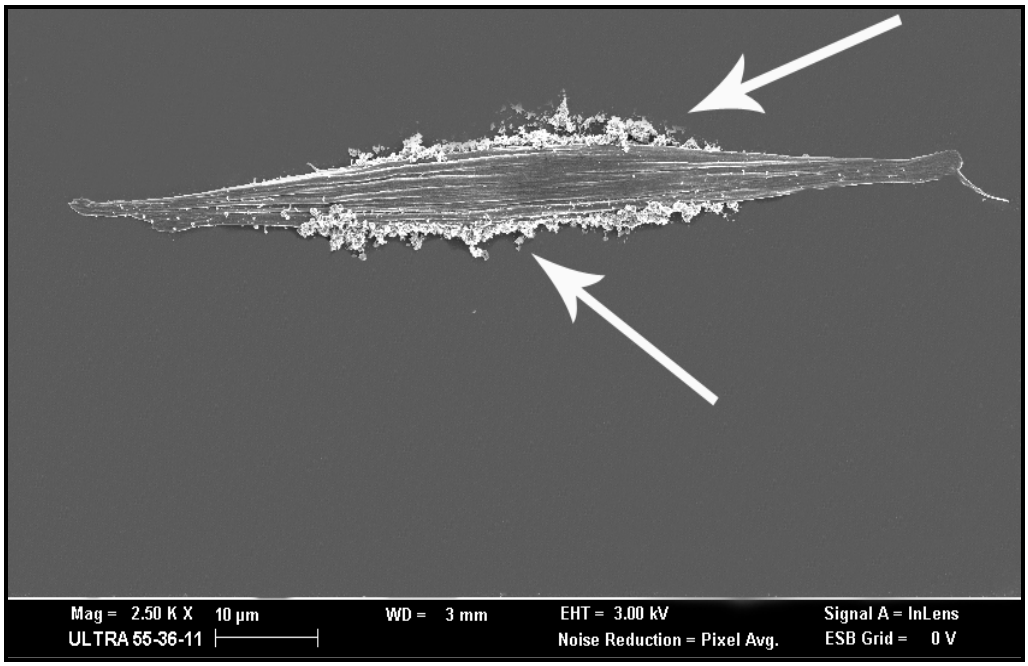

b)

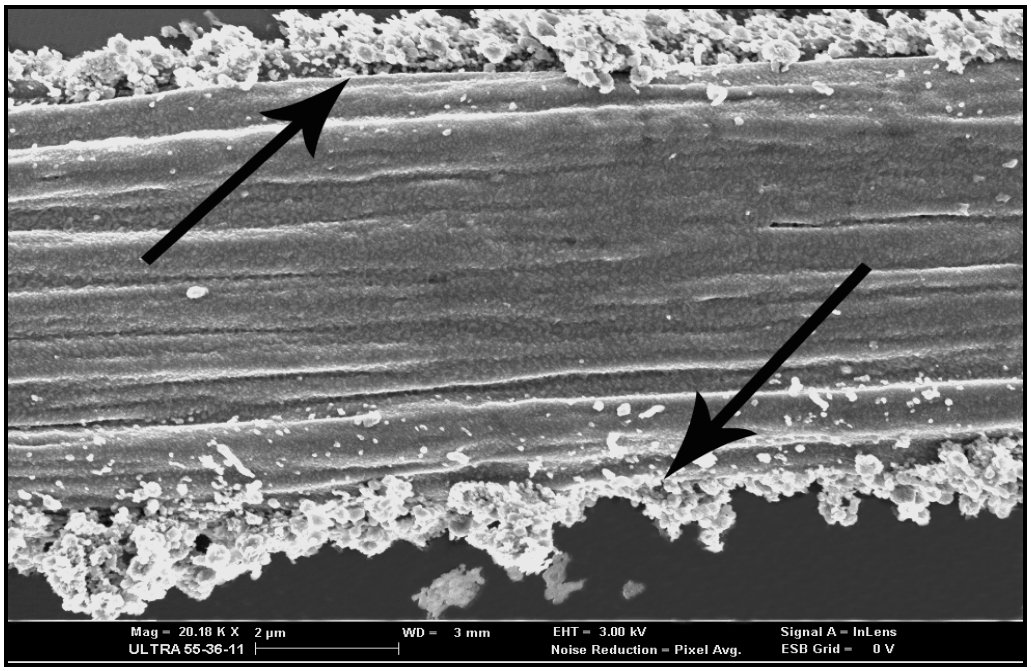

Figure 5.40: Cardiac muscle cells exposed to 0.005% Triton X-100 after pre-treatment with 0.02mg/ml CoQ10. **a**): Low magnification shows an intact cell, the white arrows indicate a presipitation on the membrane surface. **b**): Higher magnification shows an intact membrane surface. The precipitation (thick black arrows) might be derived from the protein components in the culture medium (5% foetal bovine serum).

5.4 Conclusion

To study the cellular and morphological effect of Triton X-100 and CoQ10, alone and in combination on primary chick embryonic cardiac and skeletal muscle cell cultures, scanning electron microscopy provide a powerful tool for high-resolution imaging of surfaces.

Triton X-100 has been used extensively in a wide variety of biological systems for both preparative and functional studies of membrane proteins and membrane permeabilization. In the present study we observed the solubilisation properties of Triton X-100 on membranes of primary cardiac and skeletal muscle cells in cultures. Investigation of Triton X-100 concentrations ranging from 0.5% to 0.00005% resulted in complete membrane solubilization (Figure 5.3 and 5.4) to slight shrinkage of the muscle cell membranes (Figure 5.9 and 5.11) with an indication of apoptotic process progression (Figure 5.7 and 5.8). Triton X-100 is a useful tool for investigating cytoskeletal composition and properties, as indicated by the highest two concentrations (0.5 and 0.05%) used in the study, which enabled the visualization of cytoskeletal components and variation in the cytoskeletal composition as the cell progress through the different phases of the cell cycle. Triton X-100 at 0.5% solubilizes the bilayer and most integral membrane proteins, leaving only the spectrin matrix and associated proteins in an insoluble form. Confined within this peripheral layer was a nuclear remnant. The cytoplasmic space was largely empty surrounded by a filamentous network (Figure 5.3 and 5.4). As the concentration decreased, the intensity of structural and morphological alterations was reduced. At none of the concentrations of Triton X-100 tested in the study, after 24 hours of exposure, did cells in culture show any reparative actions. No remarkable differences between the cardiac and skeletal muscle cell alterations were observed. Coenzyme Q10 (CoQ10), known to have antioxidant and membrane stabilizing properties, is the only endogenously produced lipid with a redox function in mammals. Coenzyme Q10 is necessary for adenosine triphosphate (ATP) production. Its role as a mobile electron carrier in the mitochondrial electron-transfer process of respiration and coupled phosphorylation is well established. Coenzyme Q10 has been demonstrated to scavenge free radicals produced by lipid peroxidation and prevent mitochondrial deformity during episodes of ischemia, and it may have some ability to maintain the integrity of myocardial calcium ion channels during ischemic insults. Coenzyme Q10 appears capable of stabilizing cellular membranes and

preventing depletion of metabolites required for ATP resynthesis (Greenberg *et al*., 1990 and Dallner *et al*., 2000). No cellular or morphological damage to cells were observed in the presence of the different concentrations of CoQ10 (0.2mg/ml – 0.02mg/ml) tested in the study. Cell membranes appeared smooth, intact, and most of the cells seem to be in the process of fusion or postproliferative, which might indicate that CoQ10 might enhance the proliferation process in muscle cells. Fusion of myoblasts into myotubes were seen at 0.05 and 0.01mg/ml CoQ10 (Figure 5.17 & 5.18, and Figure 5.22 &5.23), and not in any cultures exposed to Triton X-100 or in the control group, indicating that CoQ10 enhances the process of proliferation and syncytium formation in cardiac and skeletal muscle cells in culture. Membrane surfaces were remarkably smooth and intact, confirming the membrane stabilizing properties of CoQ10 discussed by Greenberg *et al*., 1990 and Dallner *et al*., 2000, with the presence of microvilli and small spherical protrusions, characterizing certain phases of the cell cycle. In all cells exposed to CoQ10, very distinct pores were visible (e.g. Figure 5.12), in some instances they appeared in larger quantities. These pores, designated “ion channels” according to the literature, are clearly activated or their function is enhanced in the presence of CoQ10 to such an extend that they appear in larger numbers in an “open” state on the surface of the cell membranes. Ion channels were present at all the concentrations of CoQ10 being tested confirming the ability of CoQ10 to maintain the integrity of myocardial calcium ion channels as described by Greenberg *et al*., 1990, Dallner *et al*., 2000, Shinde *et al*., 2005 and Terao *et al*., 2006). To determine whether CoQ10 might elicit some form of protection when cardiac and skeletal muscle cells were exposed to Triton X-100, the cultures were pre-treated with the different concentrations of CoQ10 (0.01 – 0.2mg/ml) 2 hours prior to Triton X-100 exposure at 0.05 and 0.005%. Triton X-100 at a concentration of 0.05% induced cellular and morphological alterations in the presence of CoQ10, the same as seen in the Triton X-100 group in the absence of CoQ10. We can conclude that the concentrations of CoQ10 (0.01 – 0.2mg/ml) used to pre-treat cells exposed to 0.05% Triton X-100, did not offer any protection to cells in culture. Cells exposed to 0.005% Triton X-100 after pre-treatment with CoQ10, showed membrane shrinkage (Figure 5.31) in skeletal muscle cells and membrane lyses of cardiac muscle cells (Figure 5.32) at 0.2mg/ml CoQ10. At a concentration of 0.1mg/ml CoQ10, membrane lyses were seen but the surface lamina was still present in skeletal muscle cells (Figure 5.33), while cardiac muscle cells seemed largely intact (Figure 5.34 a) at high magnification (Figure 5.34 b and 5.35). An intact membrane with bulging and a rare

appearance of a "*membrane patch"* on a part of the membrane that present more rough and slightly damaged, were seen. At a concentration of 0.05mg/ml CoQ10, skeletal and cardiac muscle cells exposed to 0.005% Triton X-100 seemed perfectly intact, with smooth membrane surfaces and the presence of ion channels. At 0.01mg/ml CoQ10 in the presence of 0.005% Triton X-100, the membrane surface of skeletal muscle cells appeared slightly shrunken, while cardiac muscle cells were intact and presented with a smooth membrane surface. The results of the study lead to the conclusion that when the concentration of Triton X-100 is too high (0.05% or higher), CoQ10 is not able to offer any protection to skeletal and muscle cells in culture. In the presence of 0.005% Triton X-100 cardiac and skeletal muscle cells showed membrane disruption and apoptotic body formation (Figure 5.7 & 5.8). When the cells were pre-treated with CoQ10 before exposure to this concentration of Triton X-100, the highest and second highest concentrations of CoQ10, showed to disrupt cell integrity, while at 0.1mg/ml in cardiac muscle cells and 0.05mg/ml CoQ10 in both cell cultures, the CoQ10 offered protection in the form of repairing cell membrane rupture by means of a "*membrane patch*" formation on the surface of the membrane where the integrity of the membrane was altered. This phenomenon was not seen in any of the other groups including the control group of the study.